3-3 Geophysical Survey

3-3-1 Purpose of survey

A transient electromagnetic (TEM) survey and Time-Domain Induced Polarization (TDIP) survey were carried out to preliminary grasp the vertical distribution of gold mineralization in the area by means of electrical resistivity and polarization.

3-3-2 Methods of survey

The TEM survey was to clarify resistivity distributions down to 150m to 200m from the earth surface and to relate the resistivity distribution to ore mineralization in the area. The TDIP survey was to find highly polarized area caused by sulfide minerals.

1) TEM Method

(1) Principles

TEM is a transient electromagnetic method, often referred to as time-domain electromagnetic method, in which the ground is energized by man-made magnetic field and its response is measured as a function of time to determine the resistivity of the earth beneath observation point as a function of depth. In this method, a steady current is passed through a loop of wire usually situated on or above the surface of the earth which is inductively linked to the earth.

The fact that loop sources, which have no direct contact with the earth, can be used makes this method suitable in areas where high surface resistivities prohibit the use of conventional direct current methods. This would include regions covered by desert, sand dunes or extrusive volcanic.

This direct current is abruptly interrupted and the secondary fields due to induced eddy currents can be measured in the absence of the primary field. The currents migrate from the transmitter into the earth and the pattern resembles a 'smoke ring'. The rate of change of the magnetic field depends upon the underground resistivity structure. For poor conductive medium, the receiver coil output voltage, which is proportional to the time rate of change of the secondary magnetic field, is initially large but decays rapidly. The response of a good conductors is initially lower but the voltage decays slower. The time derivative of the transient magnetic field which results from these currents can be measured by a coil sensor.

The decay of the secondary field measured at surface can be analyzed to determine the resistivity of the earth at depth. The resistivities of geological materials are highly dependent upon porosity, saturation, and pore fluid resistivity information about water content and its quality, and TEM resistivity measurements are a valuable structural mapping tool for groundwater studies.

The TEM method was selected for this survey for the following reasons; (1) stability of the transmitter signal, (2) lack of static shift, (3) no near field phenomena, (4) uniqueness of the results, and (5) high production rate by using ungrounded source in rock desert.

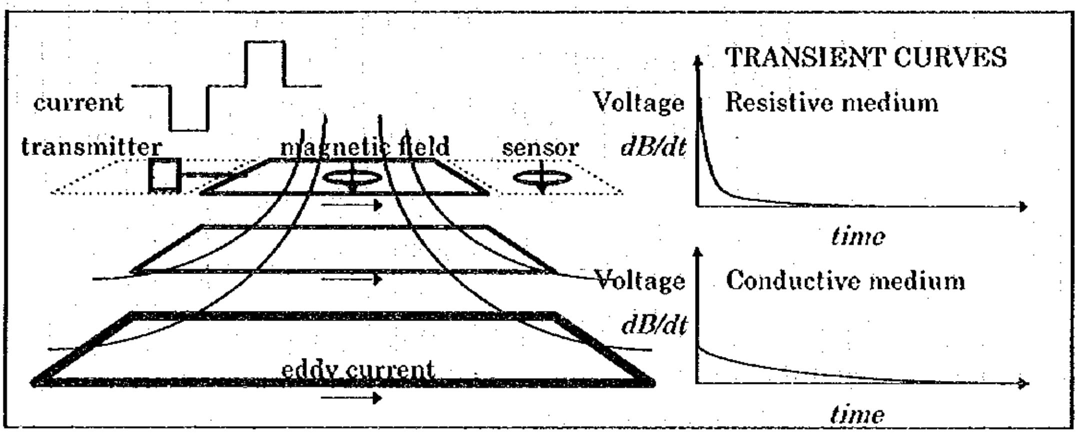

TEM survey configuration and transient curves.

(2) Equipment

The specifications of TEM measurement system manufactured by Geonics Corp., which was used in this survey, are shown in table.

The receiver console, a PROTEM (C) unit, samples the coil response to the induced magnetic field in the ground at a serious of time intervals that are displayed by a prescribed amount from each turn-off of the loop current Through the use of two transmitter-wave form base frequencies, nominally 262.5 and 25 Hz, decay voltage were recorded in two overlapping time ranges of 0.00613-0.06959 ms and 0.08813-6.978 ms, respectively, after current is turned off. There are 20 gates in each time ranges. The channel positions, or gate times, of 20 geometrically spaced time gates are shown in table.

The TEM47 is a battery-driver transmitter that can supplies a 3-ampere at the maximum. A reference cable is used to establish precise timing between transmitter and receiver.

These systems were applied to give high resolution shallow sounding up to 200 m depths.

Specifications of TEM survey equipment.

MODEL	SPECIFICATIONS	NUMBER
Receiver PROTEM(D)	Measured Quantity: Rate of decay of induced magnetic field in nV/m^2 Base Frequencies: 0.3, 0.75, 3, 7.5, 30, 75 and 285 Hz or 0.25, 0.625, 2.5, 6.25, 25, 62.5 and 262.5 Hz Time Gates: 20 geometrically spaced time for each base frequency (6 ms to 800 ms) Dynamic Range: 23 bits(132dB) Synchronization: Reference cable or high stability quartz crystal	1
Coil	Air-cored Coil Effective Area: 31.4 square meters	1
Transmitter TEM17	Current wave form: Bipolar rectangular current with 50 % duty cycle Frequencies: 30, 75, 285 Hz or 25, 62.5, 262.5 Hz Maximum Current: 3 A Output voltage: 0 to 9 V, continuously variable Turn-off Time: 2.5 μsec at 3 A into 40 x 40 m loop (Faster into smaller loop)	1

(3) Measurement

In this survey a small, square transmitter loop 40 m on a side was energized with a typical current of 2.5 A for high production rates. At each site, the receiver coil was located at the center of the square transmitter loop. The transmitter and receiver were connected by a hard wire to be synchronized. Measurements were done at high and low frequencies and stacked mostly 256 times and maximum 1,024 times for windy condition.

Sampling gate times.

GATE	BASE FREQUENCY			GATE	BASE FREQUENCY		
NO	262.5 Hz	62.5 Hz	25 Hz	NO	262.5 Hz	62.5 Hz	25 Hz
1	6.813	35.25	88.13	11	77.91	319.8	799.4

2	8.688	42.75	106.9	12	99.38	405.5	1014
3	11.13	52.50	131.3	13	126.7	514.8	1287
4	14.19	64.75	161.9	14	166.4	654.3	1636
5	18.07	80.25	200.6	15	206.0	832.3	2081
6	23.06	100.3	250.6	16	262.8	1059	2648
7	29.44	125.8	314.4	17	335.2	1349	3373
8	37.56	158.3	395.6	18	427.7	1719	4297
9	47.94	199.8	499.4	19	545.6	2190	5476
10	61.13	252.5	631.3	20	695.9	2792	6978

UNIT: μsec

(4) Data processing

Next figure shows a flow chart of data analysis used in this study. In the first phase of data processing, the decay voltages are transformed into late-time apparent resistivity values at each gates, after checking the measurement parameters (e.g., loop dimensions, gains of receiver, current, station locations and so forth) of field data.

The voltages, V_0 (in unit of mV), which are measured by the PROTEM(C) system are converted to magnetic field decay rate, dB/dt (nV/m^2), by following formula (Geonics, 1992).

$$\frac{dB}{dt} = \frac{V_0 \cdot 19200}{E \cdot 2^n}$$

where E is the receiver coil moment (m^2), and n is amplitude gain setting. Apparent resistivities $\rho_a(t)$ (ohm-m) as a function of time are then given by,

$$\rho_a(t) \cong \frac{\mu}{4 p t_c}\left(\frac{2 \mu M}{5 t_c \, dB/dt}\right)^{2/3}$$

where μ is magnetic permeability ($4p*10^{-7}$ in unit of H/m), t_c is measurement time or the gate center time in s, and M is transmitter moment which is the product of loop area (m^2) and current (A).

Occam's inversion technique, named smooth inversion, was used to generate resistivity imaging sections with up to 19 layered model. In this process, a candidate model is iteratively changed to estimate best fitting model to the observed data under restricted condition in which resistivities of each layer change smoothly. Imaging sections obtained by this technique can visualize underground structures without artificial parameterization. The imaging results were also used to estimate initial model parameters for the following one-dimensional inversion.

The one-dimensional inverse processing is used to obtain one-dimensional resistivity structures where can be assumed to be the layered model from geological point of view. In this process we can estimate structural parameters (e.g., resistivities and thickness) of best fitting models with up to 8 layers using the least squares method named automatic ridge regression.

Finally, equivalence analysis was done to estimate a set of equivalent models, that is, alternative models that fit the data nearly as well as the best-fit model, but differ from this model. The forward calculations for each model are used; these are selected to determine the extent to which modifications to the model can be made according to these guidelines without exceeding a user-specified error. Equivalence analysis also indicates the allowable range of each of the model parameters.

The program which we have used in this study is "TEMIX-GL" developed by Interpex Ltd.

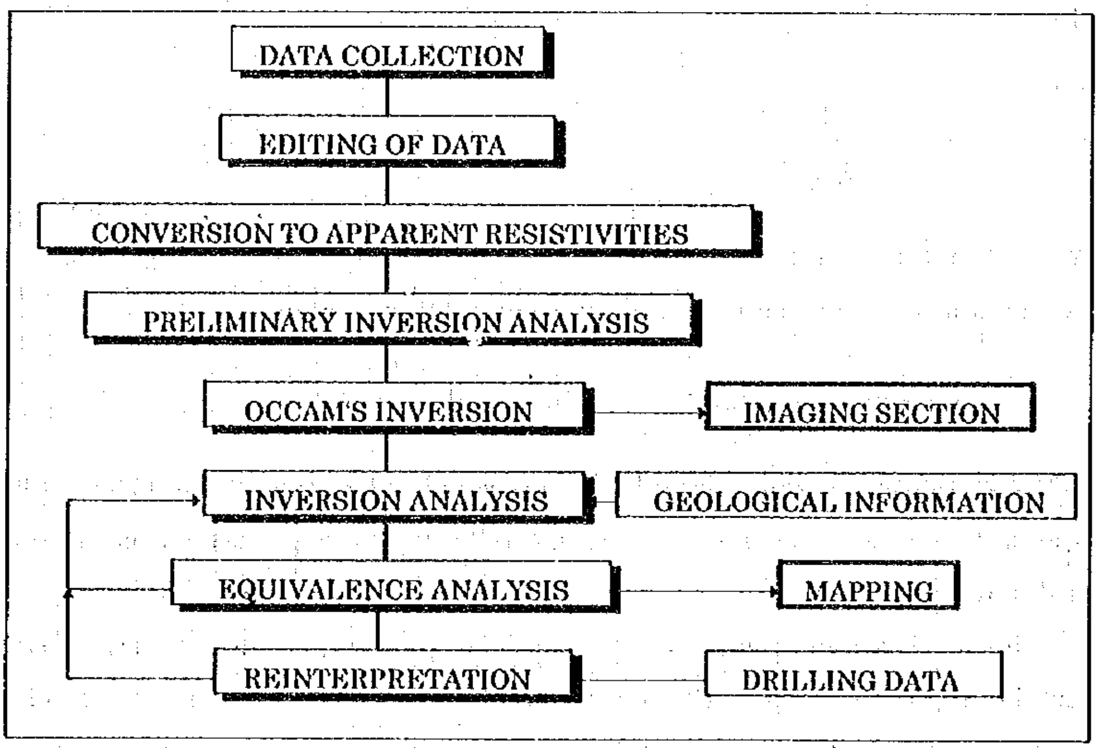

A flow chart of data analysis

2) TDIP Method

(1) Principles

Induced Polarization method, usually abbreviated IP method, is an electrical exploration method involving measurement of the slow decay of voltage in the ground following the cessation of an excitation current pulse.

Induced polarization phenomena, also known as overvoltage, is caused by electrochemical process when electrical current passes through metallic minerals where phase of conduction changes ionic to electronic.

For the current survey TDIP method was used to delineate distributions of sulfide minerals.

(2) Equipment

The specifications of TDIP measurement system manufactured by Zonge Engineering Co., which was used in this survey, are shown in the following table

Generator	Gasoline Engine Generator ZMG-7.5 Output power: 7.5 kW, 400Hz, 3 phase
Transmitter	Transmitter GGT-6 Maximum output: 6 kW, 24 A, 1000 v, DC ~ 10 kHz
Controller	Transmitter Controller XMT-16 Controlled frequency range: DC ~ 10 kHz
Receiver	Geophysical Data Processor GDP-16 Data processor: amplification, A/D conversion, data processing Frequency range: DC ~ 8 kHz

(3) Measurement

In this survey, gradient array, shown in the following figure, is used.

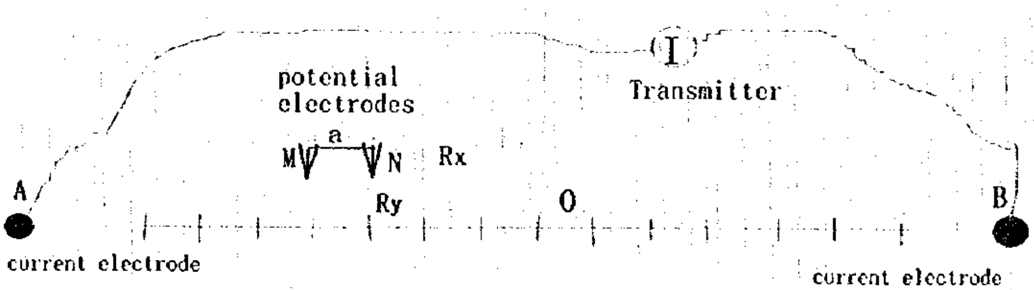

Apparent resistivity is calculated by the following equation.

$$\rho_a = 2\pi a \cdot K_{xy} \cdot V / I$$

where

$$K_{xy} = [\{(m+n-1)^2 + p^2\}^{-1/2} - \{(m-n+1)^2 + p^2\}^{-1/2} - \{(m+n)^2 + p^2\}^{-1/2} + \{(m-n)^2 + p^2\}^{-1/2}]^{-1}$$

V : measured voltage, A : transmitted current

m :: $AB/2a$, n : R_x/a, p : R_y/a

Time domain IP measurements record decay voltage after primary DC current being turned off. Decay voltage is recorded as 1,024 separate windows in few seconds after current being shut off. Chargeability (M), an index to show IP effect, is calculated as a time integral of secondary decay voltage curve.

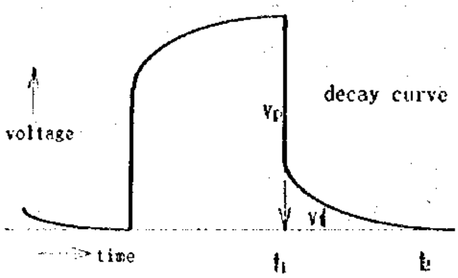

$$M = \frac{1}{V_p} \int_{t_1}^{t_2} V t\, dt$$

(4) Measurement

Before taking measurement, we tested electromagnetic coupling between source cable and receiving cable, and decided to use frequency of 0.125 Hz (8 seconds period) and integrate decay curve between 0.45 second and 1.10 second after termination of primary current (Newmont standard approximation).

In order to avoid electromagnetic coupling between source and receiver cables, the both cables were separated at least 250m.

Receiving electrode separation was 20 m throughout the survey.

(5) Data Processing

Chageabilty of this survey is normalized by the following equation.

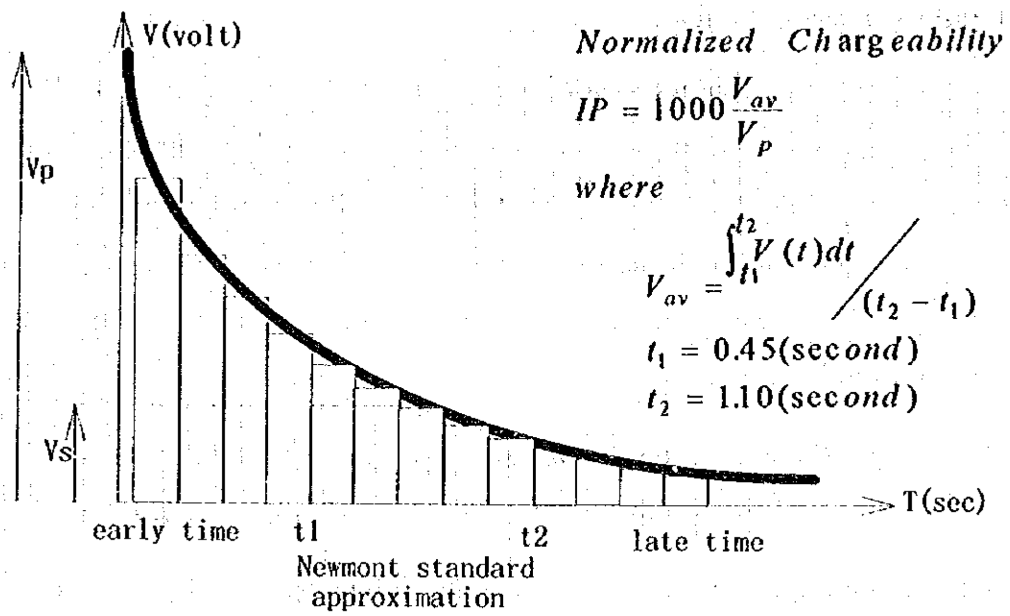

3-3-3 Results of survey

The location of survey lines and stations are shown in Fig. II-3-3-1(1) and (2). Due to the presence of buildings over the Bulutkan ore deposit, part of Line-2 has been displaced to the east.

In explanation of the results, resistivity and IP values shall be classified as follows :

[Resistivity]

under 10 Ωm	Very conductive (layer)
10 to 100 Ωm	Conductive (layer)
100 to 1,000 Ωm	Medium resistivity (layer)
1,000 to 10,000 Ωm	Resistive (layer)
over 10,000 Ωm	Very resistive (layer)

[IP]

under 40 mV/V	Low IP
40 to 60 mV/V	Medium IP
over 60 mV/V	High IP

1) Resistivity Structure Sections

Resistivity sections along the survey lines are presented in Fig. II-3-3-2(1) through (10). Earth resistivities are represented by colored zones in these figures. Reddish colors designate areas of low resistivity and bluish colors imply areas of higher resistivity.

The resistivity section is similar along all of the survey lines. The sections can be divided into southern, central and northern structural zones. The features of these three zones are as follows:

<u>"Southern structural zone"</u>: Medium to resistive layers are present from the surface to depth in this zone. There are also discrete resistive to very resistive bodies.

<u>"Central structural zone"</u>: This zone is generally conductive. There are, however, medium to resistive layers, 10 to more than 100 m thick, at the surface in some places. There are also some small bodies with medium to high resistivies in this zone.

<u>"Northern structural zone"</u>: The structure in this zone consists of three layers. There is a conductive layer, about 100 m thick, at the surface, underlain by a very conductive layer and a less conductive basement.

The resistivity structures along the survey lines are summarized in Table II-3-3-1.

In the vicinity of the Bulutkan ore deposit (Line-2), there are continuous, resistive to very resistive, bodies at depth.

2) Resistivity structure map

The resistivity structure maps are compiled at three levels, 200 m above sea level, 150 m above sea level and 100 m above sea level, Fig. II-3-3-3(1) to (3).

The distribution of resistivities are very similar at all three levels. Resistivity values are high in the south and decrease to the north. The general features of the resistivity distribution are as follows:

i) Medium to resistive layers dominate the southern part of the survey area. The lateral extent of these layer is greatest at 200 m above sea level where they occupy about one half of the survey area. The medium to resistive layers are less extensive at 150 m above sea level and their distribution is about the same at 100 m above sea level.

ii) On the east side of the Bulutkan ore deposit, there is a resistive zone which runs from WNW to ESE at 200 m and 150 m above sea level.

iii) At 200 m above sea level, there are several small, very conductive zones. These merge into one large conductive zone which trends from WNW to ESE at 100 m and 150m above sea level.

3) IP section

Apparent resistivity values and IP values, calculated from data collected with potential electrode separations of 20 and 40 m, are shown in Tables II-3-3-2(1) through (6) and Fig. II-3-3-4(1) through (6).

IP data profiles are similar along all of the IP survey lines. Chargeability values are low, about 35 mV/V, from station 0 through station 14 to 20, at the south end of lines. IP values become medium to high in the north. The stations at which the IP chargeability boundary falls on each of the survey lines and zones of anomalously high chargeability are summarized in the following table.

Line	Line-1	Line-2	Line-3	Line-4	Line-5	Line-6
IP boundary	No.16	No.20	No14.	No.16	No.16	No.20
High IP area	No.35-47 No.52-63	No.32-35 No.47-82 No.97-100	No.57-81	No.56-66	No.43-54	No.30-58

IP values around the Bulutkan ore deposit are about 45 mV/V. These values are anomalously high in a region of medium IP chargeabilities.

4) Apparent resistivity map

A map of apparent resistivity at a potential electrode spacing of 40 m is shown in Fig. II -3-3-5. The apparent resistivity is low in the northern part of the survey area, including some zones of apparent resistivity under 10 Ωm, and high in the southern part of the area.

The apparent resistivity distribution is similar to that derived from the TEM resistivity data.

5) IP Chargeability Distribution Map

An IP chargeability distribution map, at a potential electrode spacing of 40 m, is presented in Fig. II -3-3-6. There is a low IP zone in the southern part of the survey area, a high IP zone in the central survey area, and a zone of medium IP chargeability in the north. IP equipotential lines in the survey area trend WNW-ESE. There is a zone of very high IP chargeability (more than 60 mV/V) which runs from WNW to ESE through the center of the survey area.

6) Physical properties of rock samples

The resistivity and IP chargeability of rock samples from the survey area have been measured in laboratory tests and the results are presented in Table II -3-3-3. The mean of resistivity and IP chargeability are following, syenodiorite is 14,200 Ωm and 4 mV/V, sulfide vein is 1 Ωm and 240 mV/V, and altered rocks are 9,000 Ωm and 89 mV/V.

3-3-4 Conclusive summary and consideration

1. Geophysical survey summary

TEM and TDIP surveys were carried out to study the resistivity and polarization of the earth and to delineate zones of prospective gold deposition in the survey area. These surveys resulted in clarification of the resistivity of the earth to a depth of 200 m and the near surface IP chargeability in the survey area.

The results of these surveys can be summarized is as follows:

i) The survey area can be divided into three zones of consistent resistivity structure.

ii) "Southern structural zone" In the southern part of the survey area there are mainly layers of medium to resistive from the surface to depth.

iii) "Central structural zone" The central survey area is conductive with surface layers of medium to high resistivity occurring locally. These surface layers vary in thickness from 10 m to more than 100 m, in some places.

iv) "Northern structural zone" The resistivity structure consists of three layers in the northern part of the survey area. There is a conductive layer, about 100 m thick, at the surface. This is underlain by a second layer which is very conductive and a third layer of moderate conductivity.

v) The IP chargeability is low (under 30 mV/V) in the southern part of the survey area and high in the central survey area. A very high IP anomaly (over 60 mV/V) extends from the WNW to the ESE through the center of the survey area. At the boundaries of the high and low IP zones, the IP equipotential contours are very dense.

vi) There is good agreement between the TEM resistivity map and the IP apparent resistivity map.

These results have been integrated into a "Geophysical Interpretation Map", Fig. II-3-3-7. In this map the following features should be noted.

a. high resistivity and low IP chargeability in the southern structural zone,

b. high IP chargeability in the central structural zone,

c. resistive zones, ① through ⑤, in the central structural zone,

d. a conductive zone in the northern structural zone,

e. dense IP equipotential lines forming a boundary in the southern and central structural zones.

The boundary between the southern and central structural zones nearly coincides with a dense IP equipotential line boundary. This boundary clearly reflects a change of the underground geological structure. The boundary at depth dips northward, from the west border of the survey area to Line-4, and dips southward east of Line-4.

The surface geology in the southern structural zone is dominated by the occurrence of syenodiorite. From this, we may infer that the extent of the southern structural zone reflects primarily the distribution and structure of syenodiorite.

2. Relation of the geophysical results to mineralization

The Bulutkan ore deposit is composed of silica veins bearing gold mineralization. The drill survey revealed the presence of *Kokpatas* formation sandstone, slate and limestone and their metamorphosed hornfels, and skarn in the areas surrounding the deposit. Laboratory resistivity and IP tests of rock samples from the Bulutkan area shows that the Bulutkan ore deposit is resistive with high IP chargeability. The results of the field survey show the same physical properties to exist around the Bulutkan ore deposit. Therefore, when exploring this area for ore deposits similar to the Bulutkan deposit, we must pay attention to resistive bodies with high IP chargeability.

The geophysical survey revealed that the Bulutkan deposit indicates high resistivity and high IP chargeability, located in the central structural zone near the southern structural zone. The resistive structure continues from the surface to depth with IP values of 40 to 50 mV/V.

Zones of prospective ore deposition, similar to the Bulutkan ore deposit, must fulfill the following conditions. In the central structural zone, prospective areas must be resistive or very resistive and IP chargeability values must be high (over 40 mV/V).

Drill hole MJUB-6 revealed that a very high IP anomaly (over 60 mV/V) in the central structural zone is a reflection of sulfide mineralization (mainly pyrite), and that the anomalous area has almost no ore bearing potential. Resistive zones, shown in Fig. II-3-3-7 as ① to ⑤, in the central structural zone have potential of bearing ore deposits like Bulutkan. The location of these five zones within the survey area and relative to survey lines can be described as follows;

① is a resistive zone in the southwestern survey area, which includes the Bulutkan ore deposit. This zone is intersected by Lines 1 through 4

② is in the center of the survey area and is intersected by survey Lines 3 and 4,

③ is north of ① and is intersected by lines 2 and 3,

④ Is an eastward continuation of ②, intersected by Lines 6 and 7,

and,

⑤ is in northwestern survey area and is intersected only by Line-2.

Resistive zones,① through ③, are relatively large and are continuous to depth, but resistive zones ④ and ⑤ are relatively small and shallow.

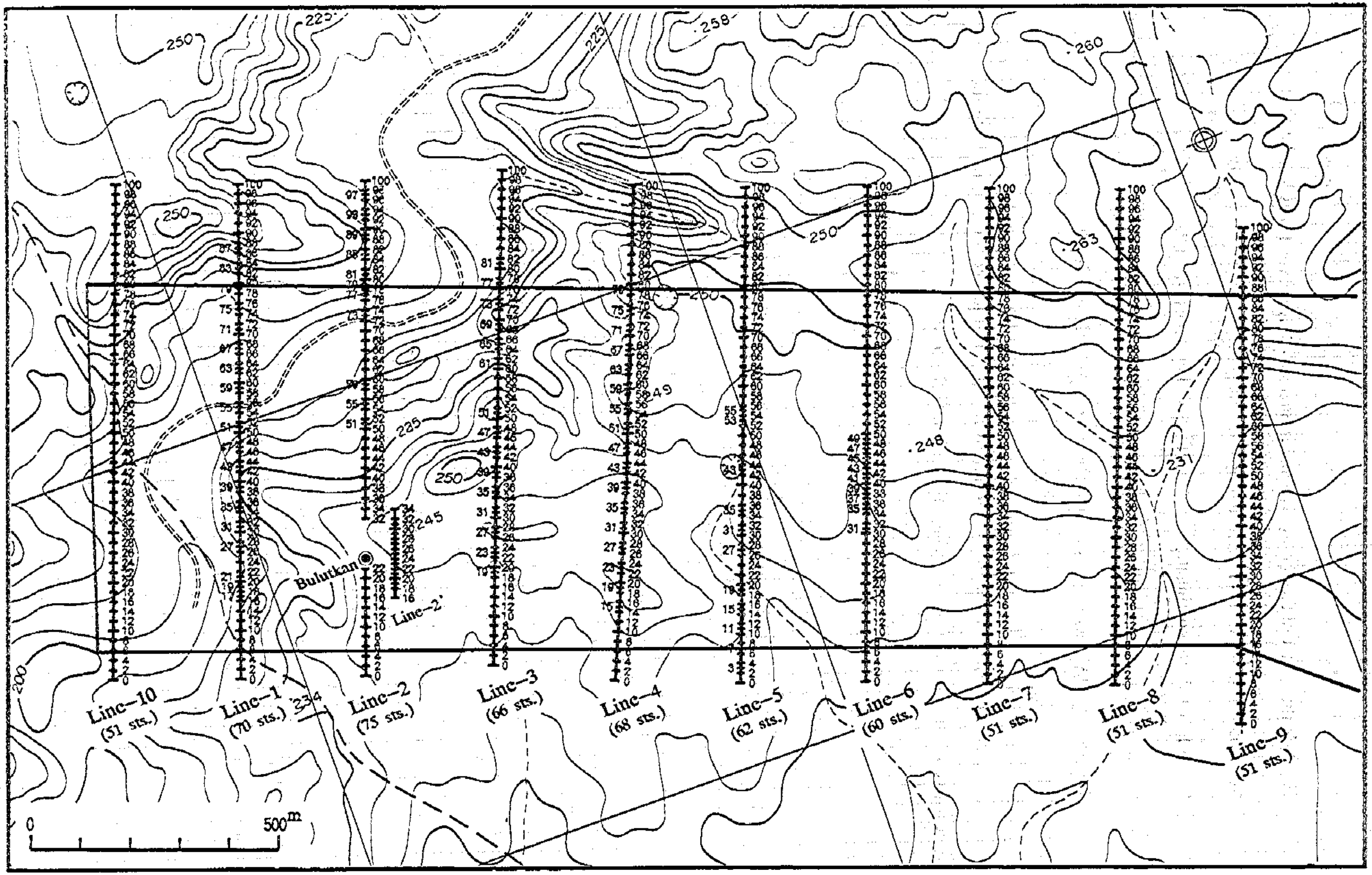

Fig.II-3-3-1(1) Location Map of TEM Survey Lines and Stations

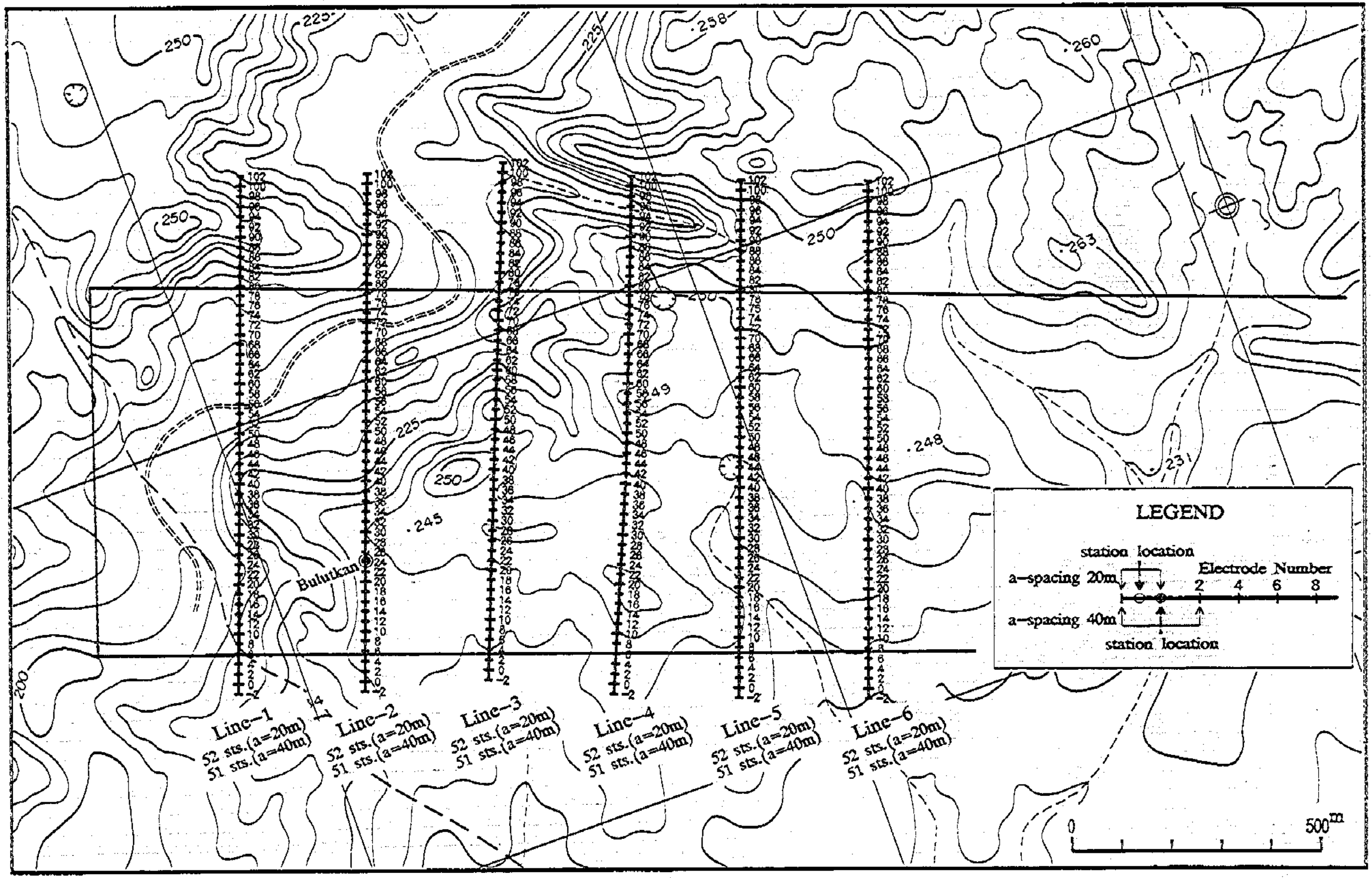

Fig.II-3-3-1(2) Location Map of TDIP Survey Lines and Stations

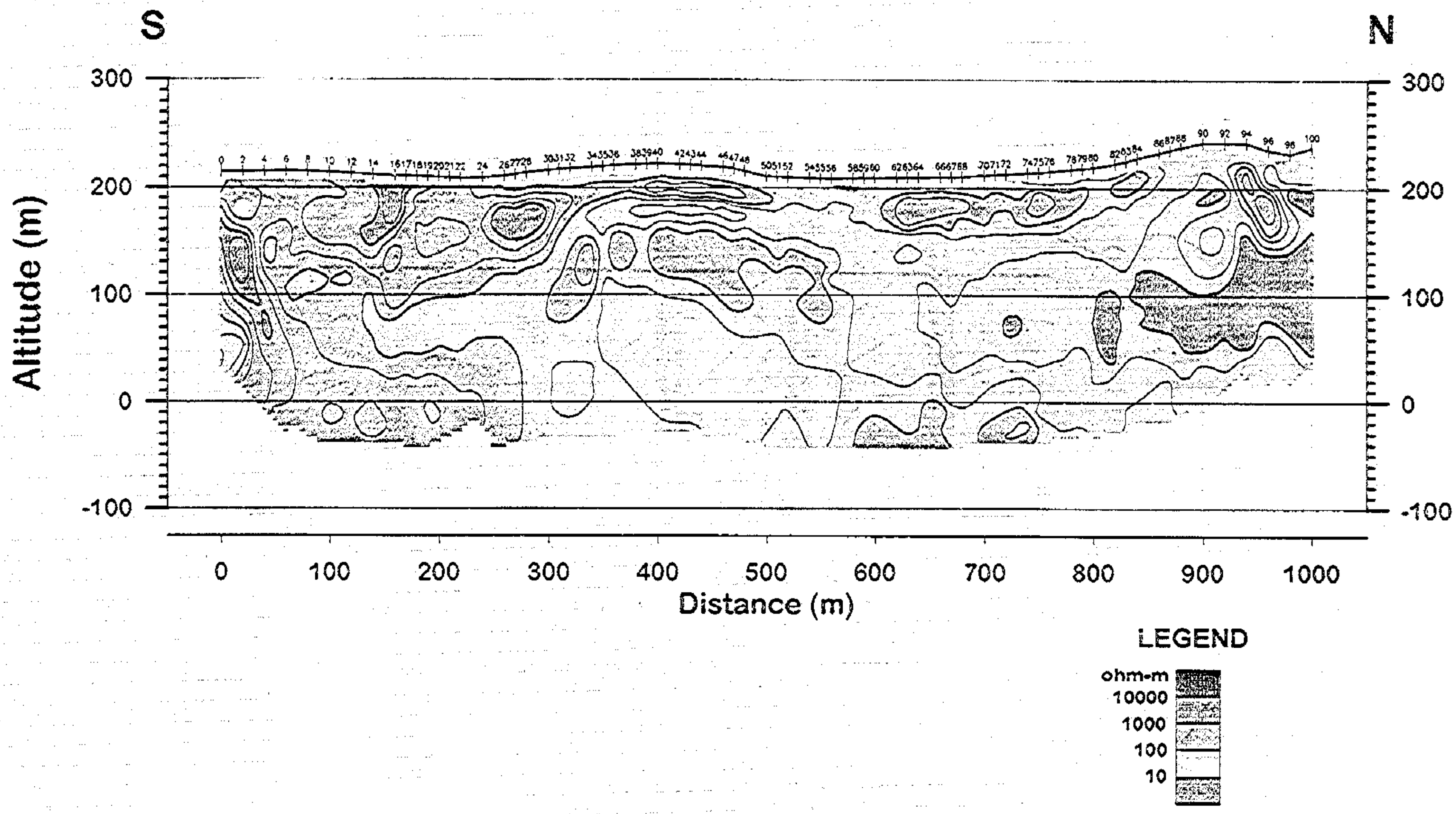

Fig.II–3–3–2(1) Resistivity Structure Section (TEM Line–1)

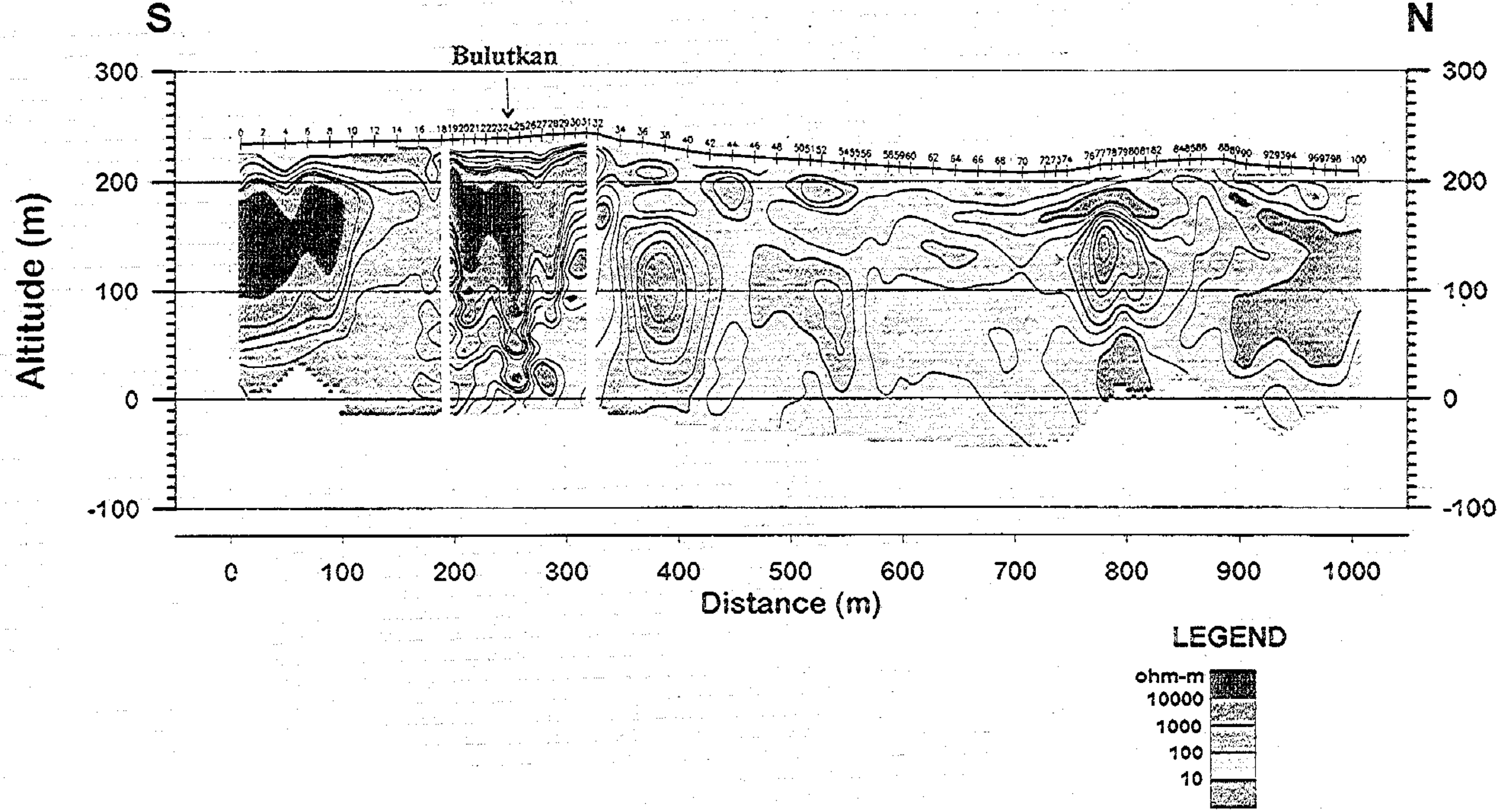

Fig.II-3-3-2(2) Resistivity Structure Section (TEM Line-2)

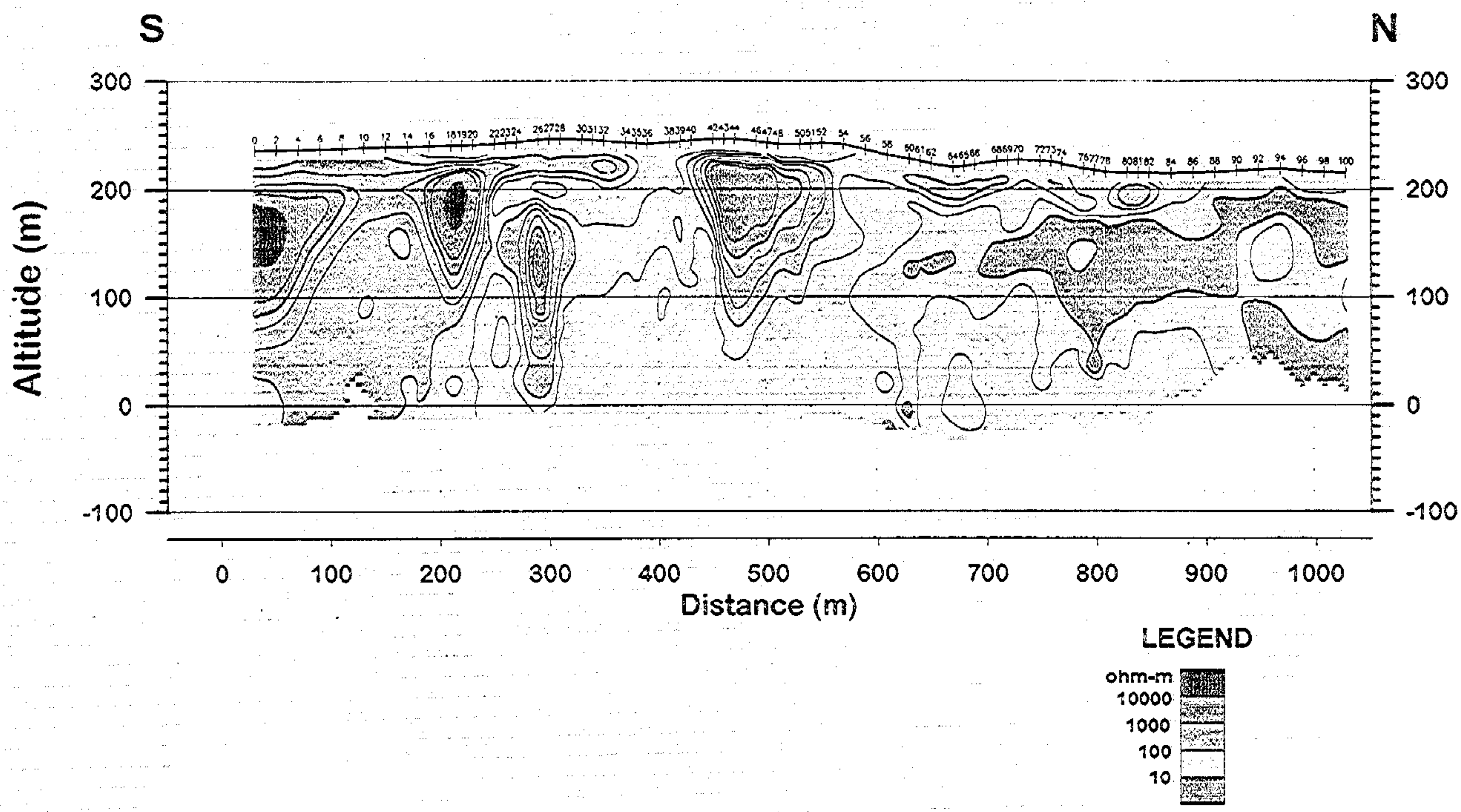

Fig.II–3–3–2(3) Resistivity Structure Section (TEM Line–3)

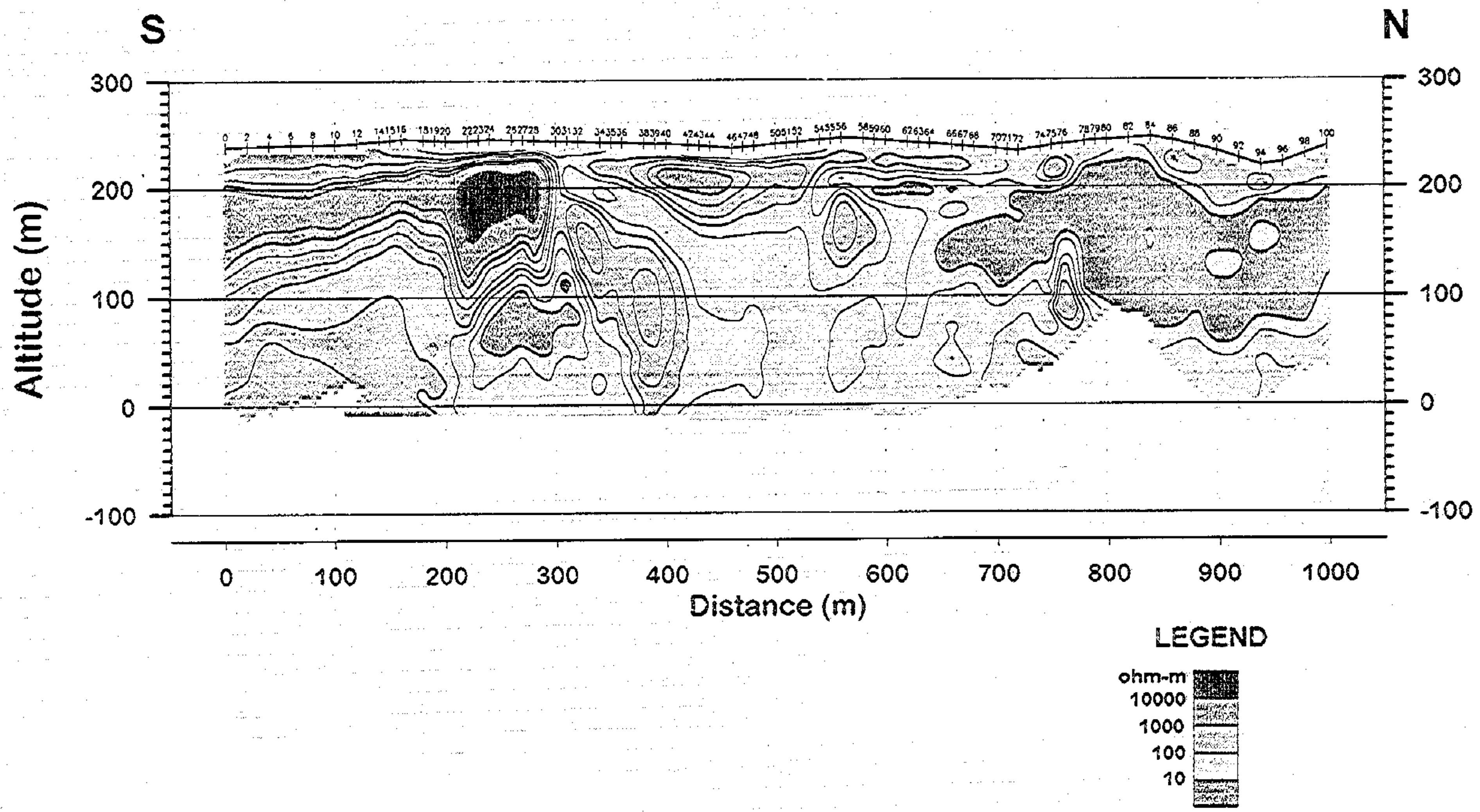

Fig.II–3–3–2(4) Resistivity Structure Section (TEM Line–4)

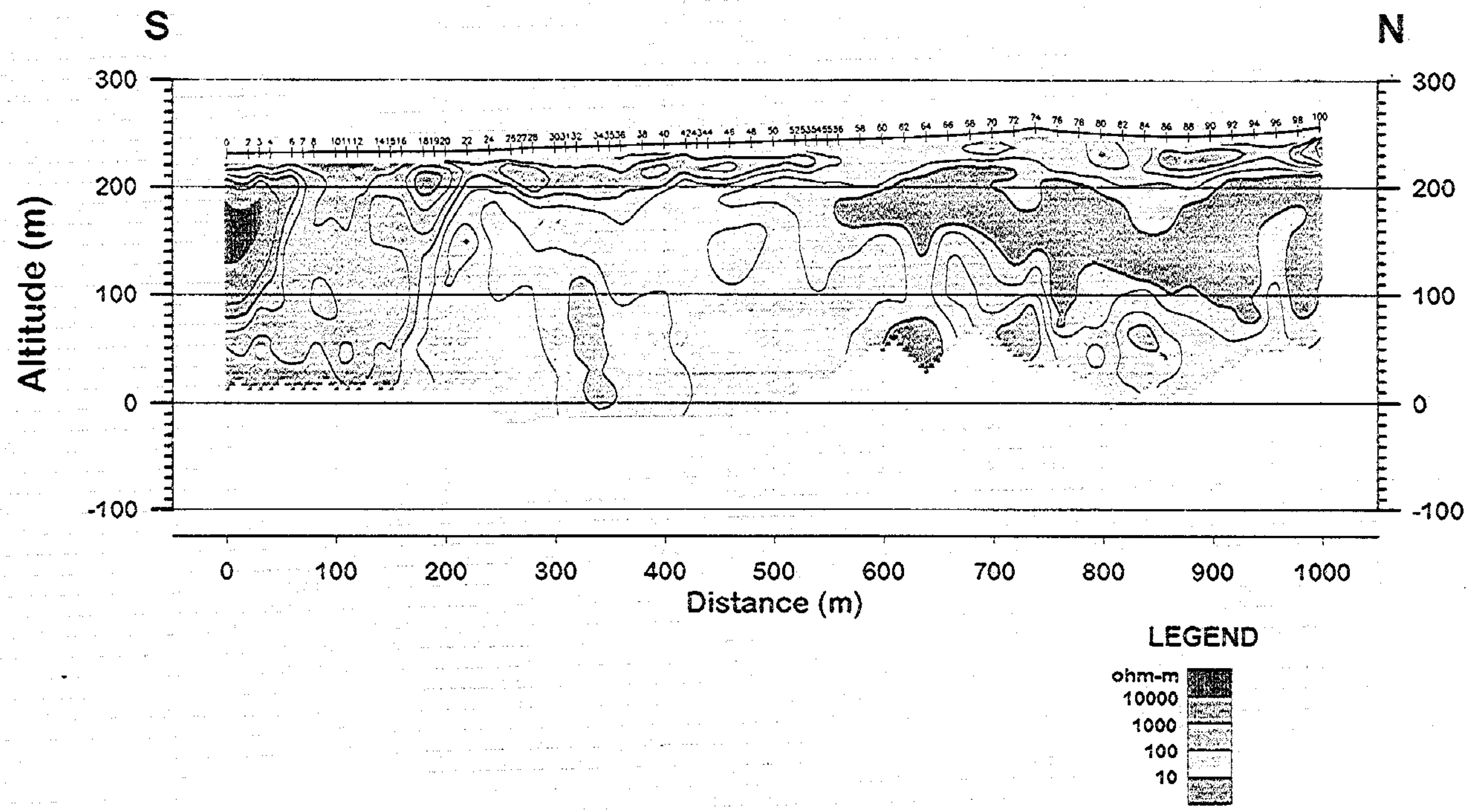

Fig.II–3–3–2(5) Resistivity Structure Section (TEM Line–5)

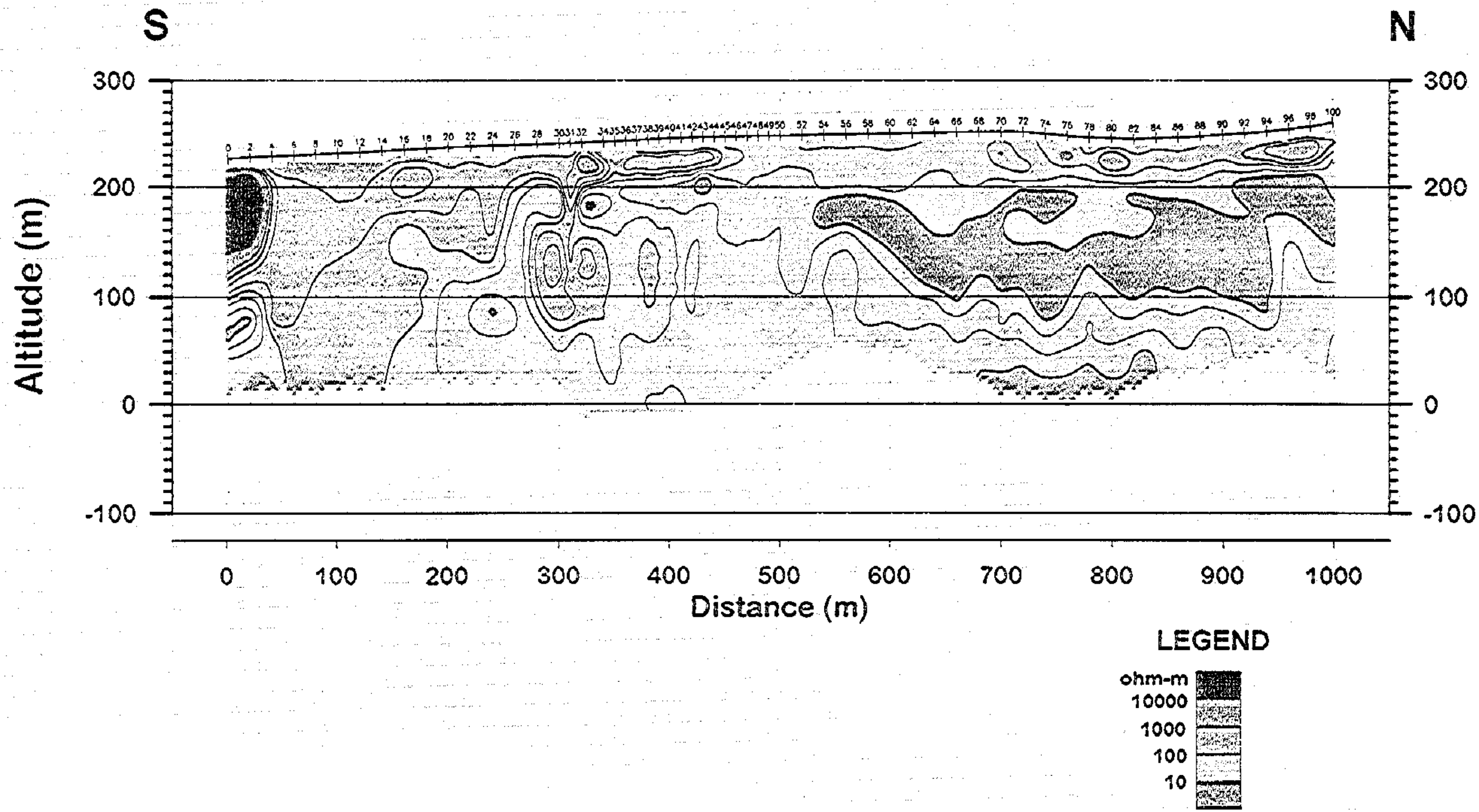

Fig.II-3-3-2(6) Resistivity Structure Section (TEM Line-6)

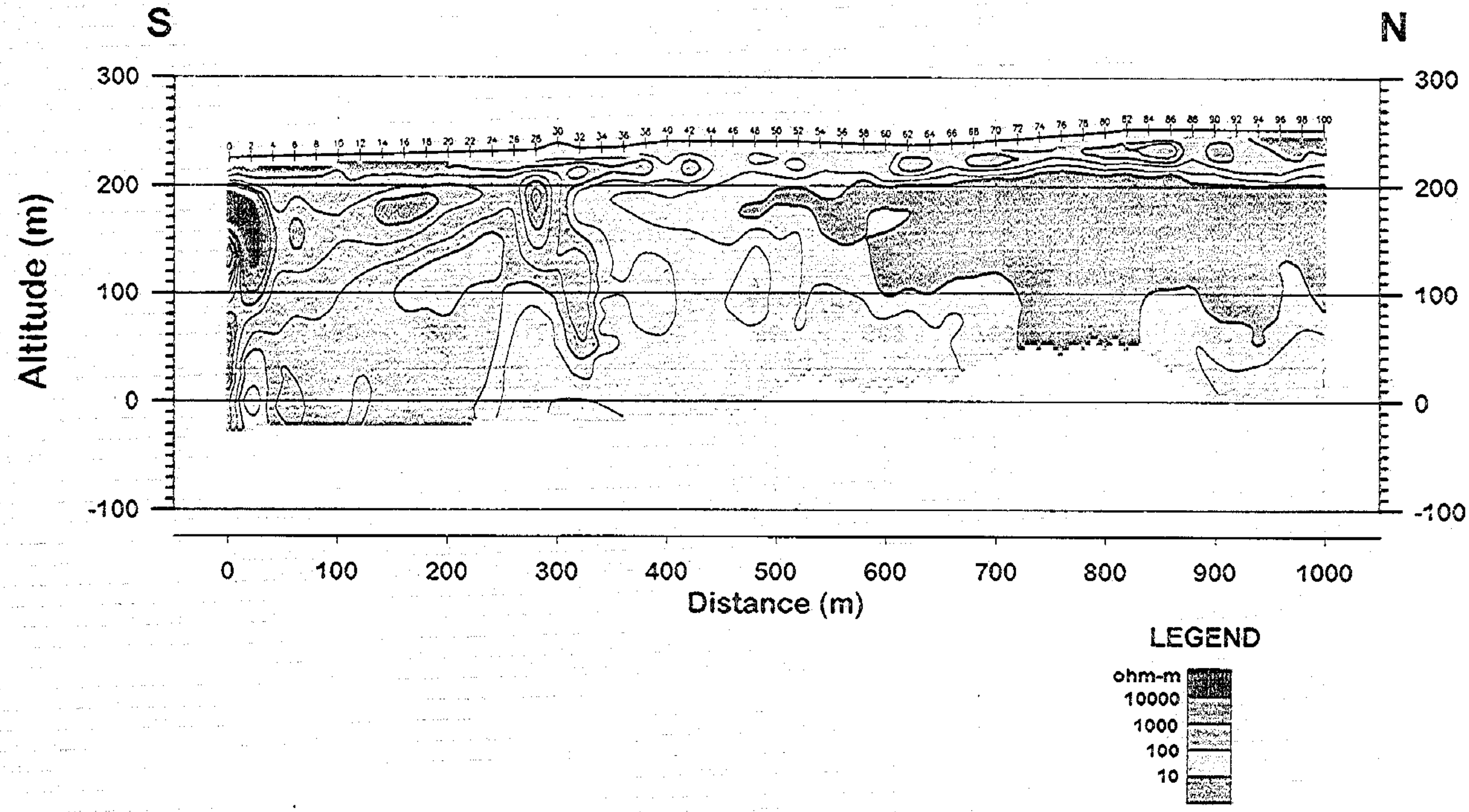

Fig.II-3-3-2(7) Resistivity Structure Section (TEM Line-7)

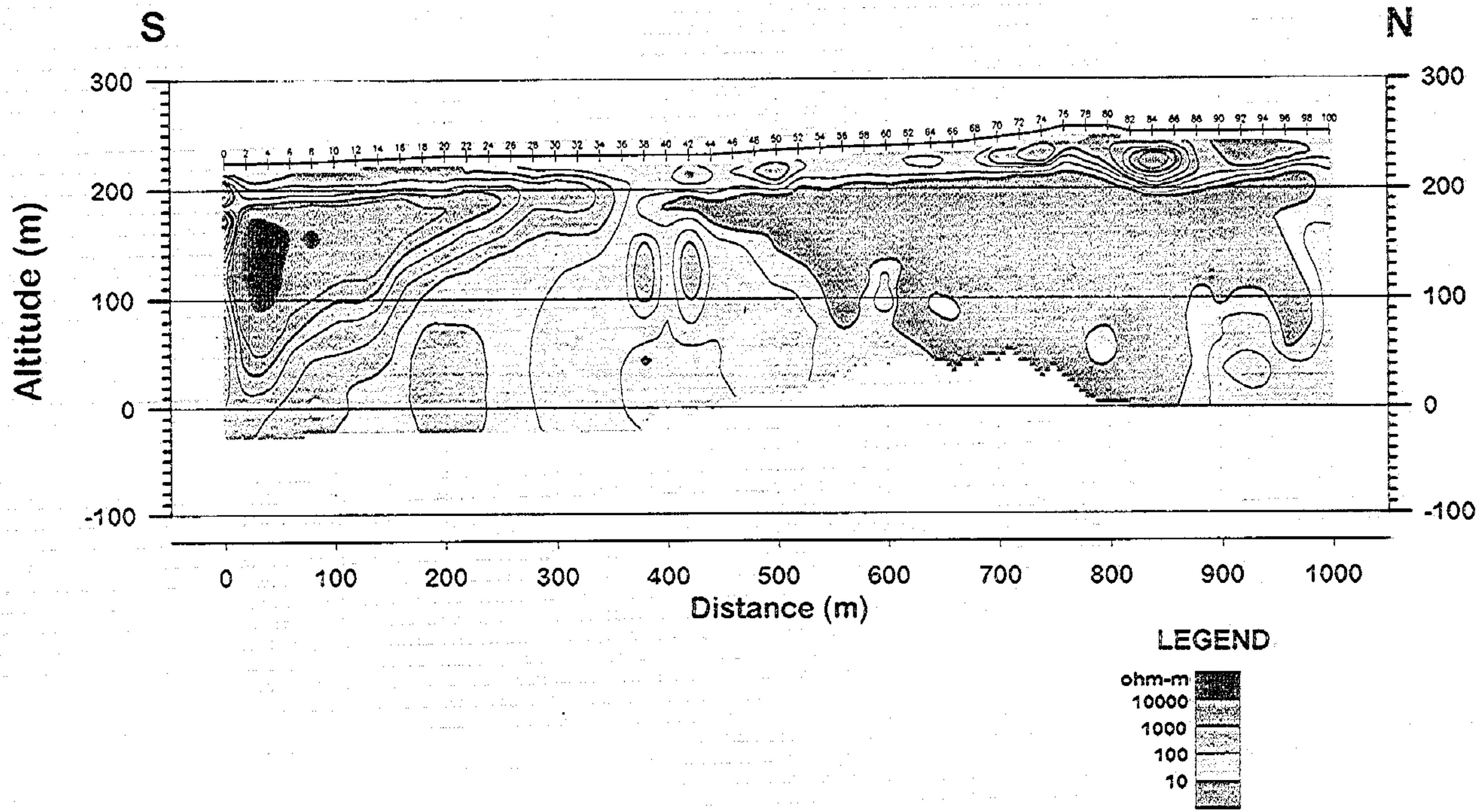

Fig.II–3–3–2(8) Resistivity Structure Section (TEM Line–8)

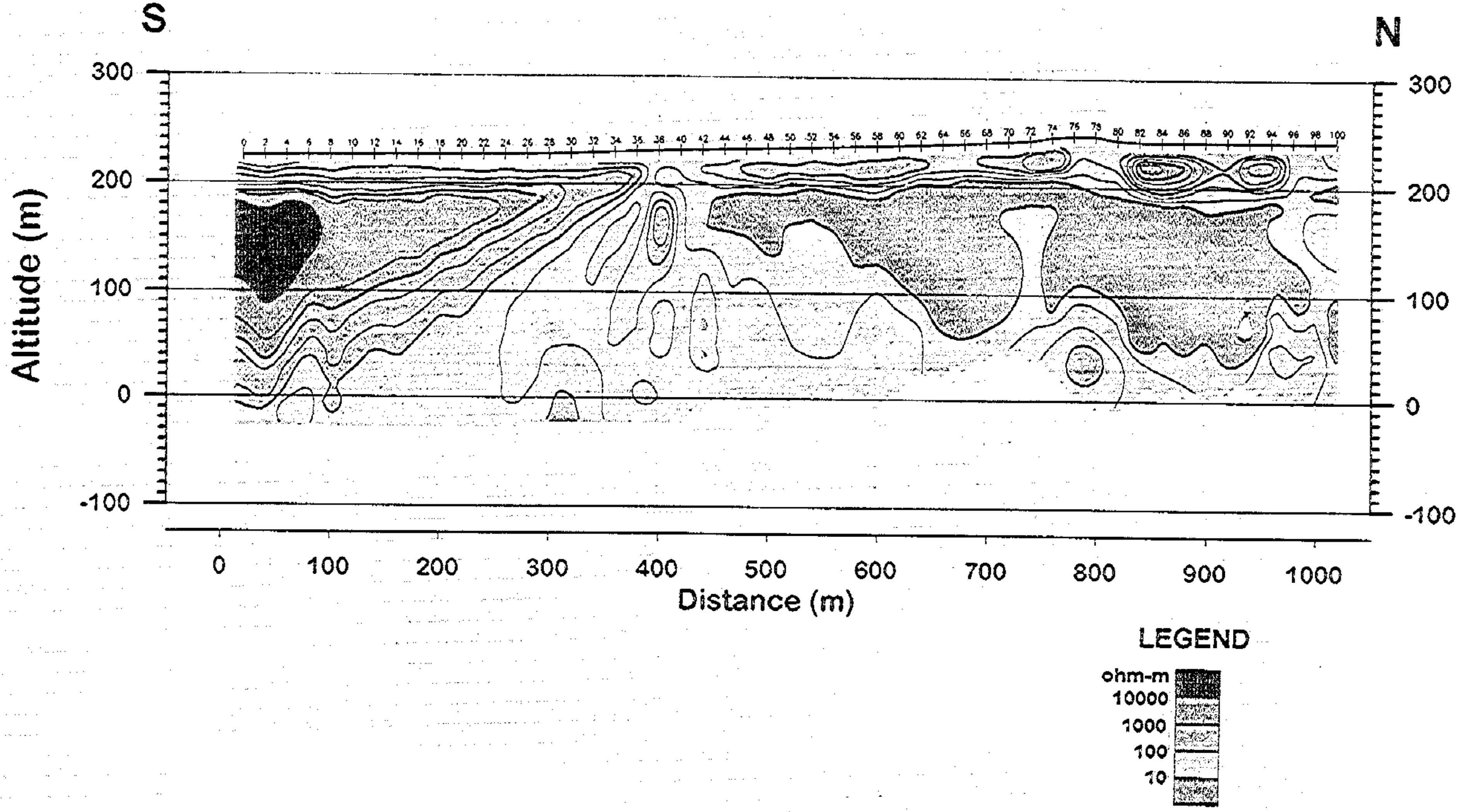

Fig.II–3–3–2(9)　Resistivity Structure Section (TEM Line–9)

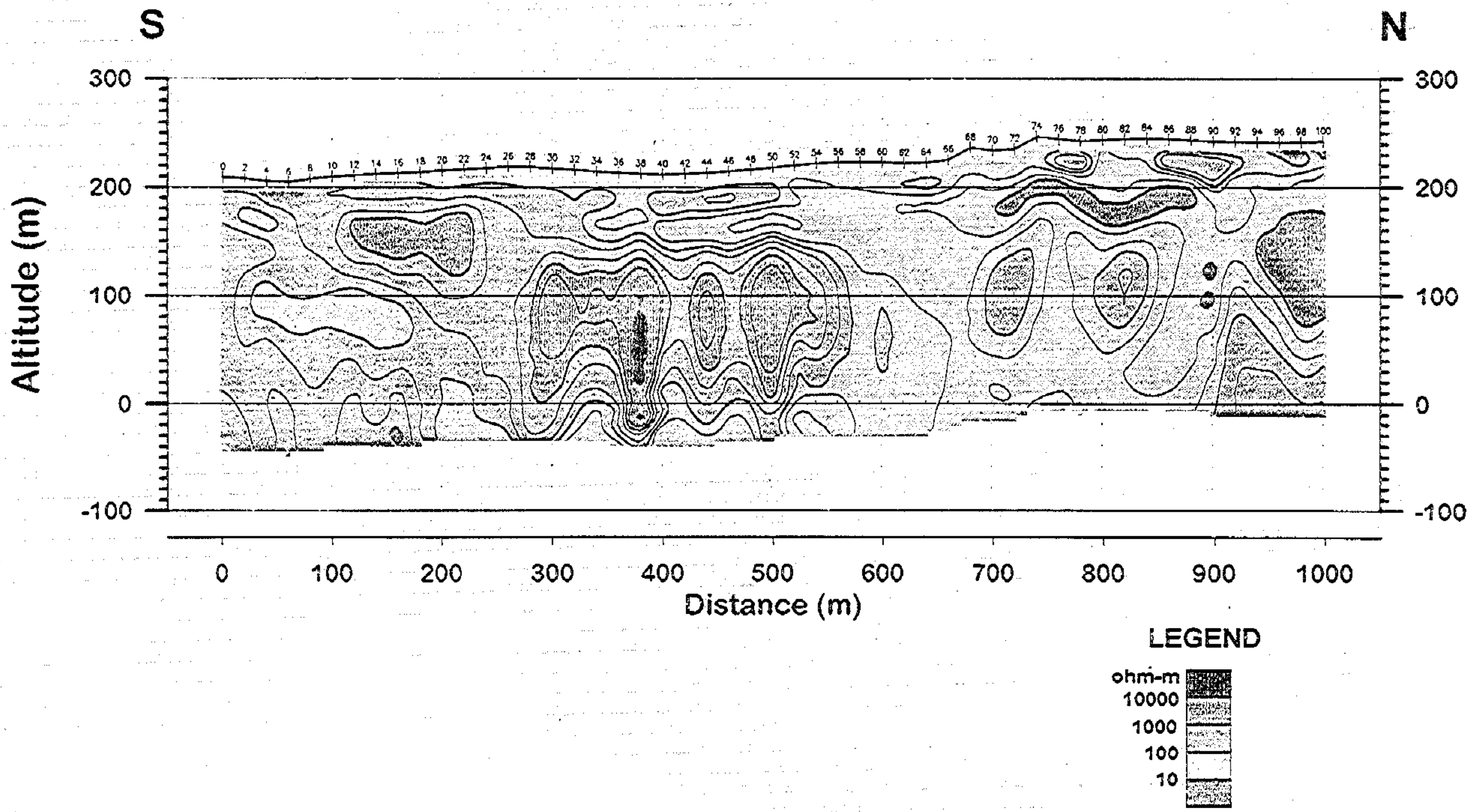

Fig.II–3–3–2(10) Resistivity Structure Section (TEM Line–10)

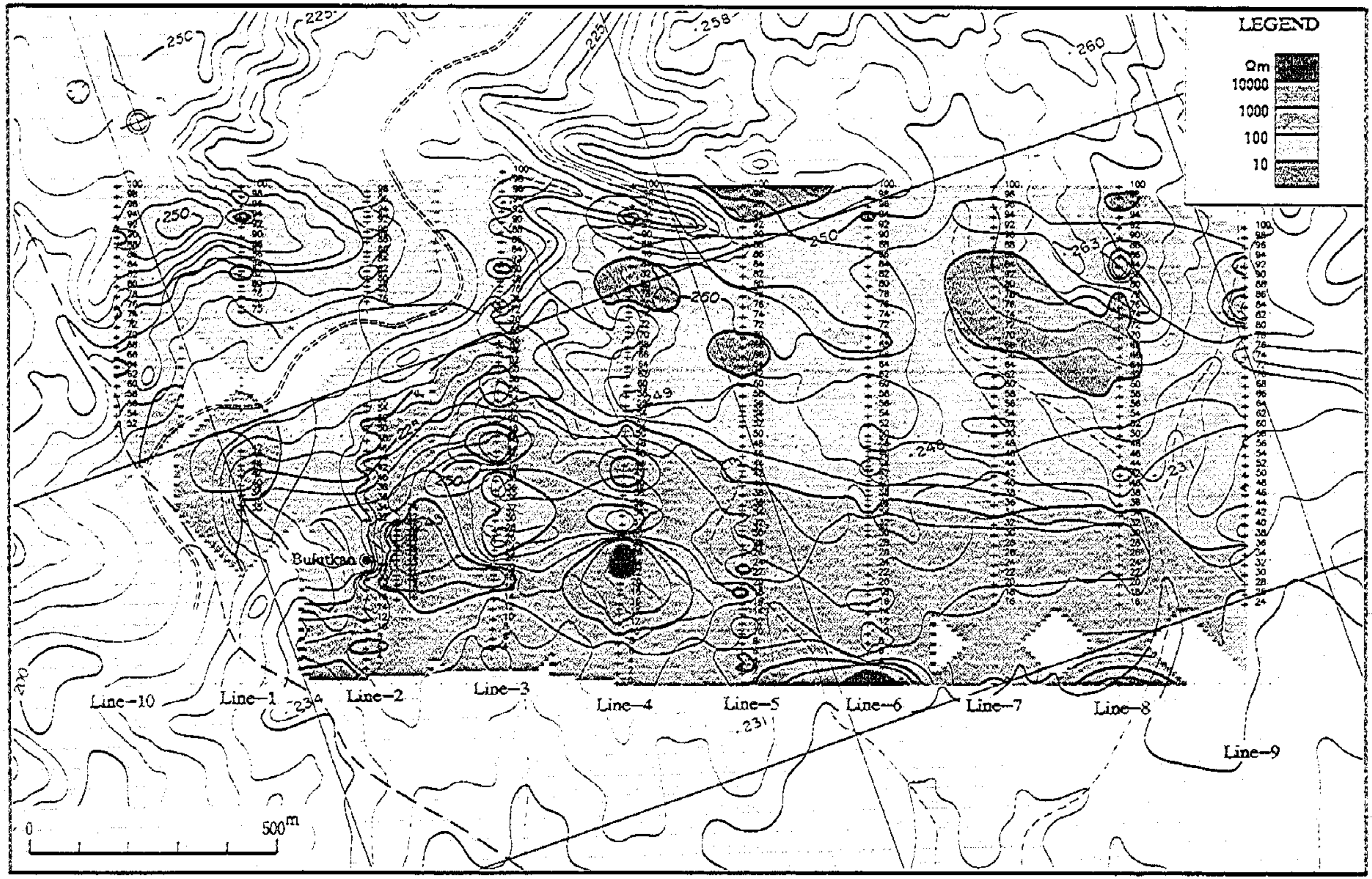

Fig.II-3-3-3(1) Resistivity Structure Map (200m A.S.L.)

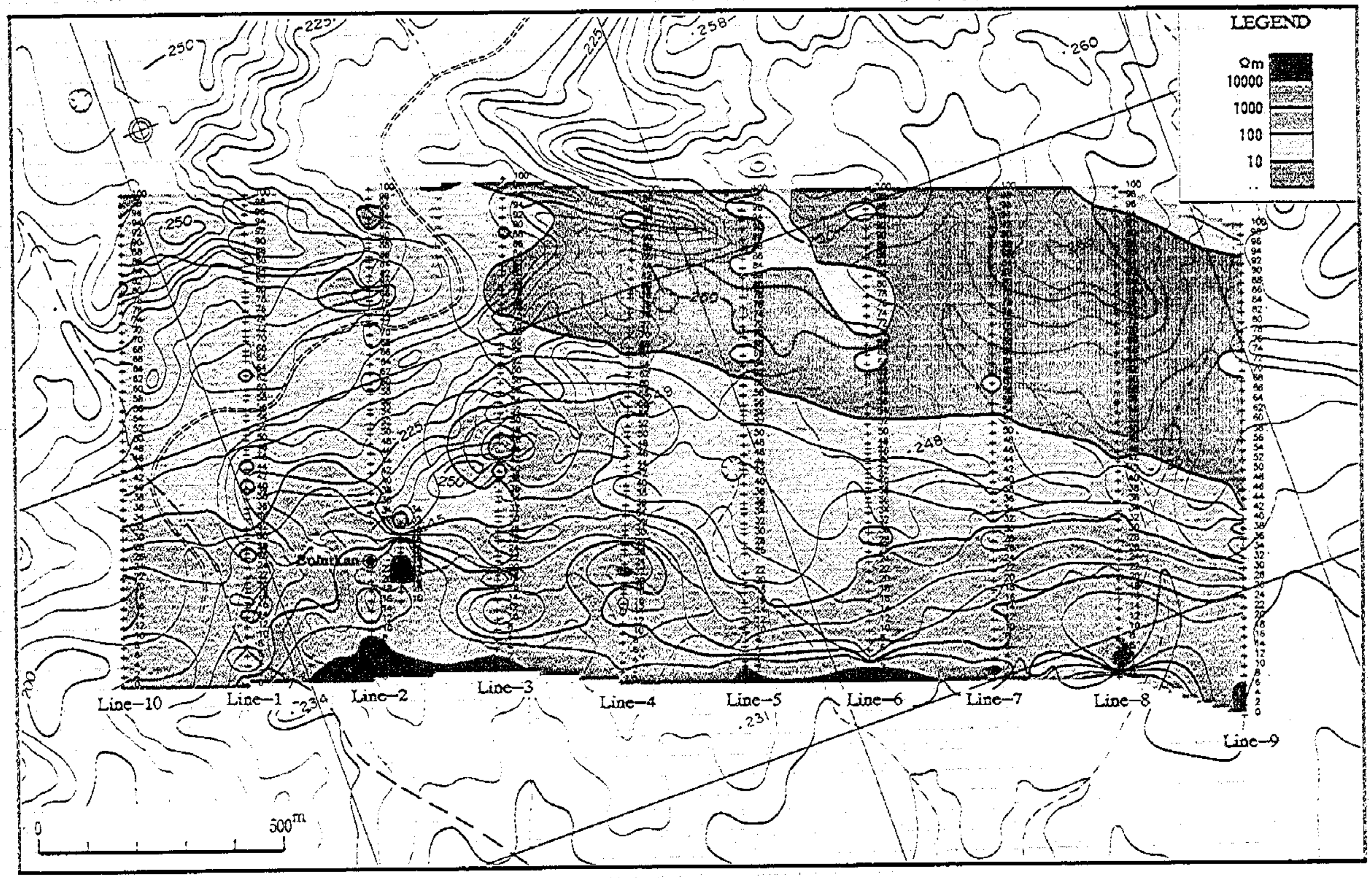

Fig.II-3-3-3(2) Resistivity Structure Map (150m A.S.L.)

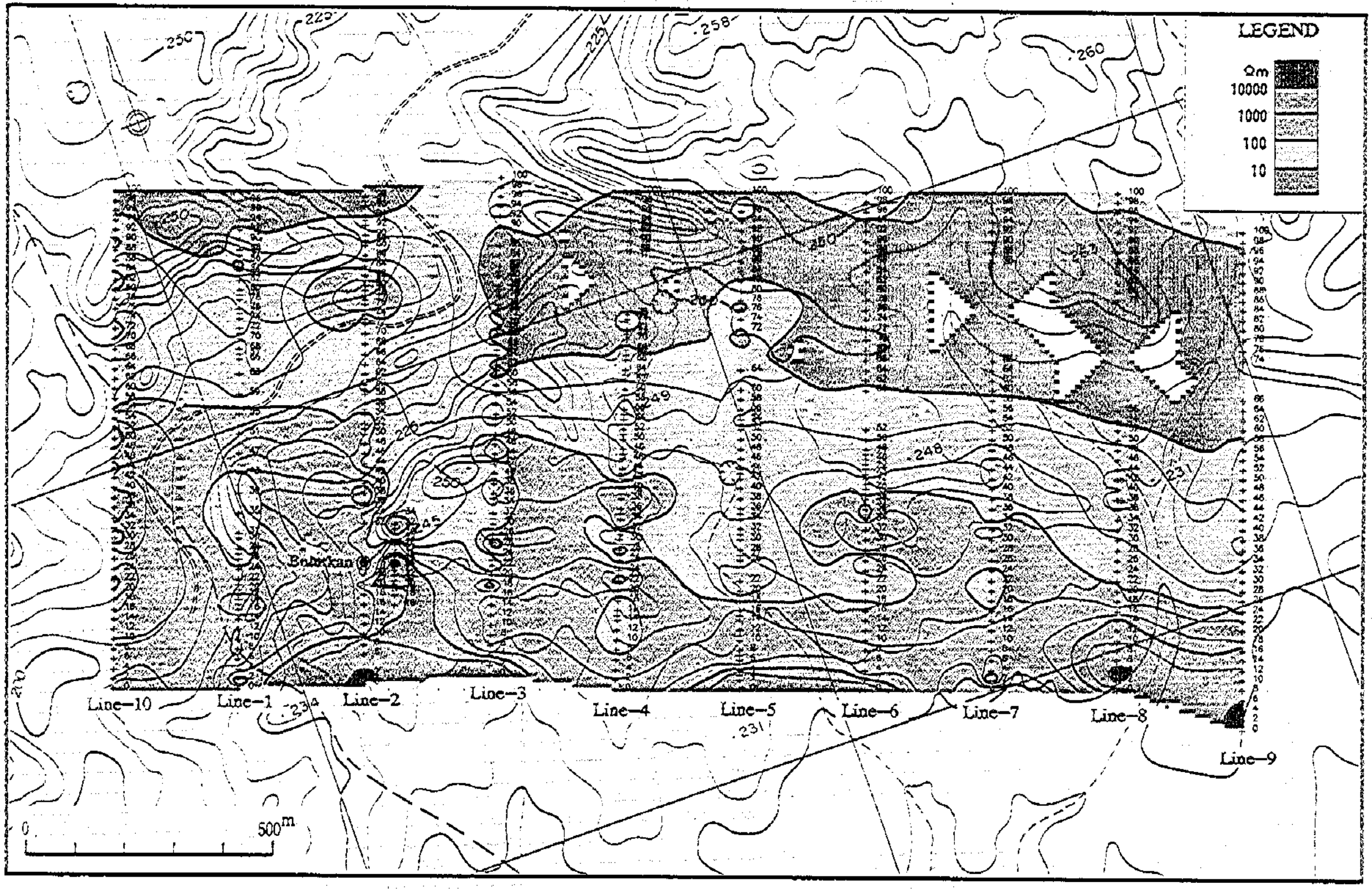

Fig.II-3-3-3(3) Resistivity Structure Map (100m A.S.L.)

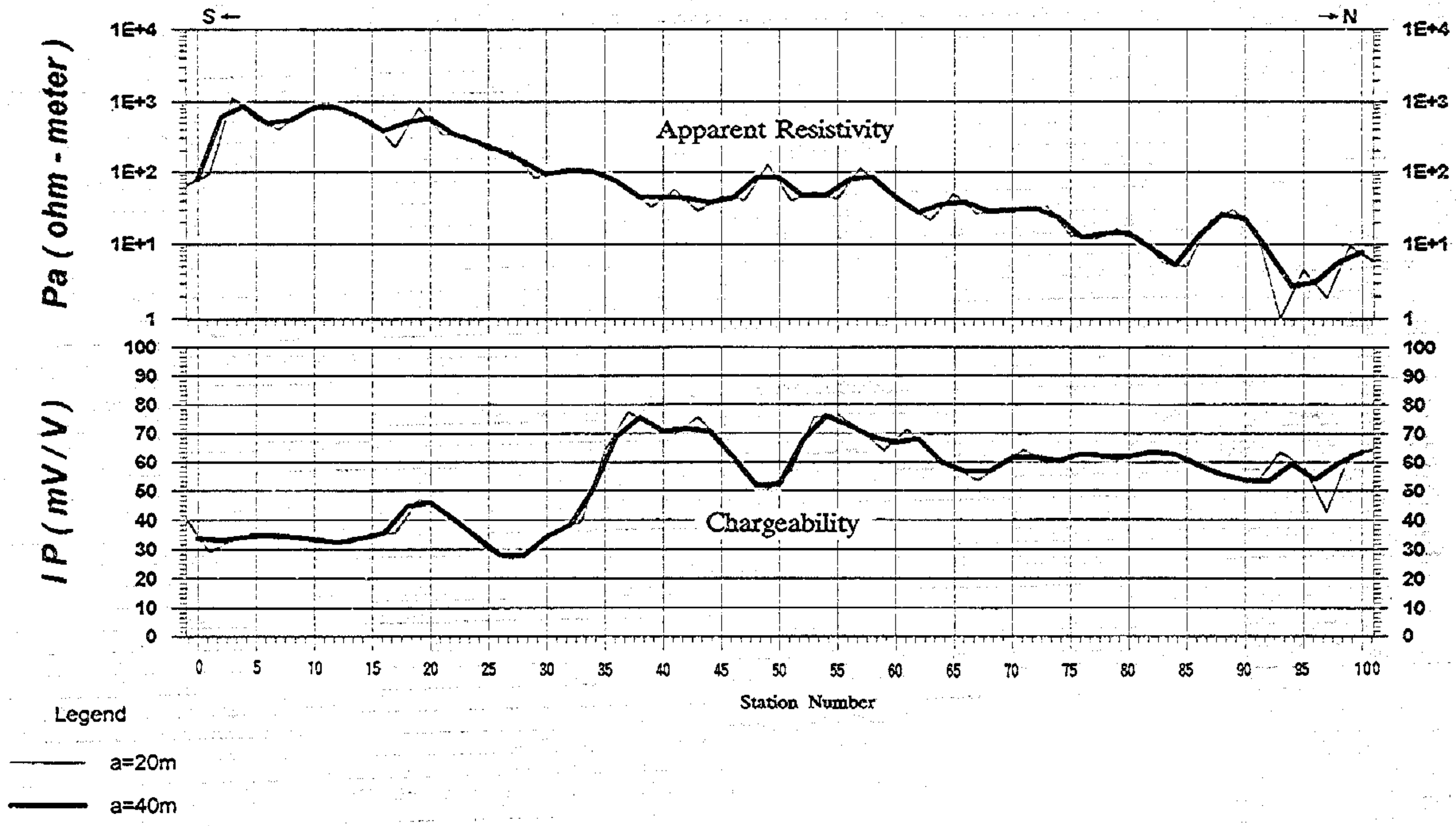

Fig.II–3–3–4(1) Apparent Resistivity and Chargeability Section (TDIP Line–1)

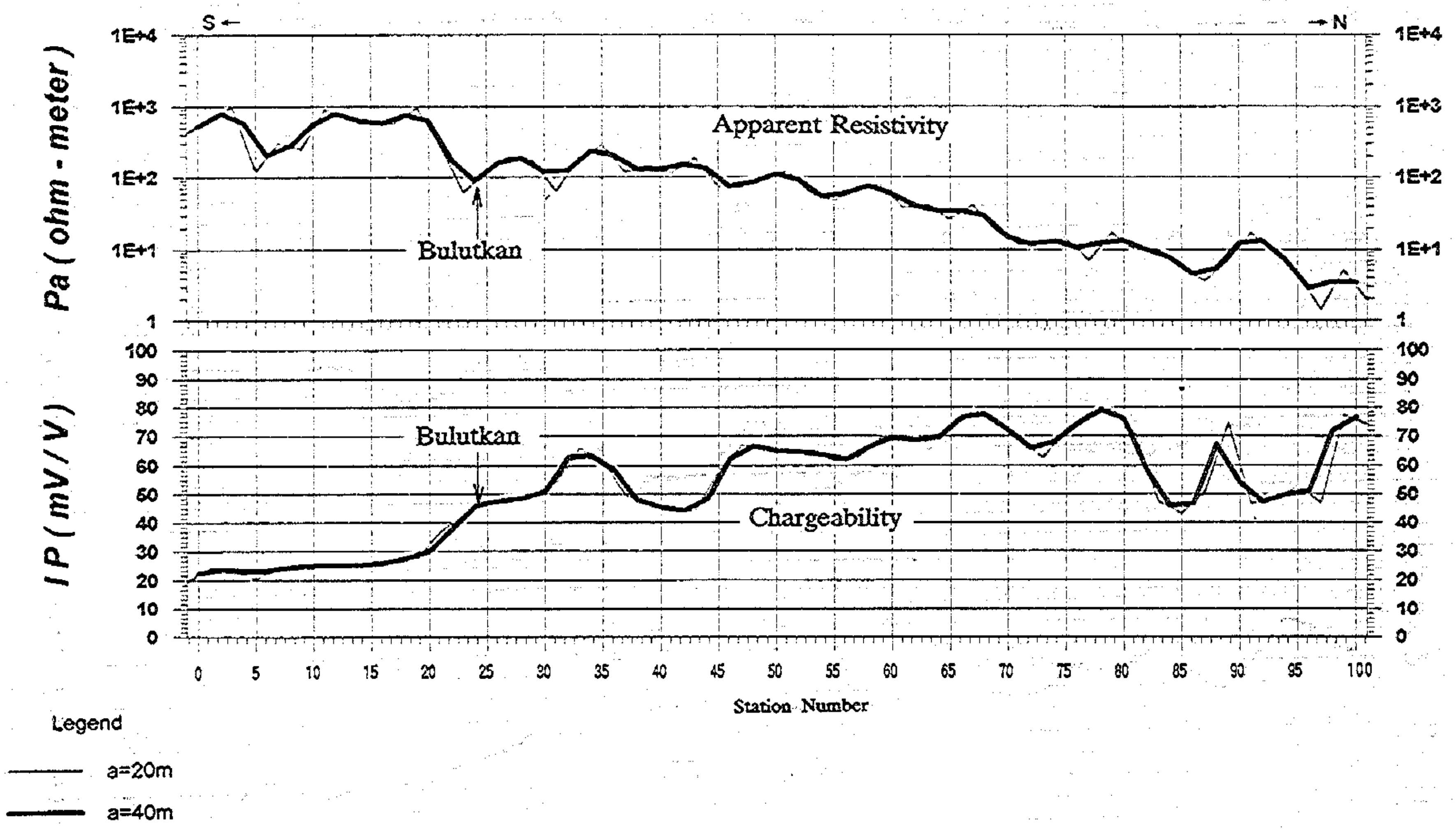

Fig.II–3–3–4(2)　Apparent Resistivity and Chargeability Section (TDIP Line–2)

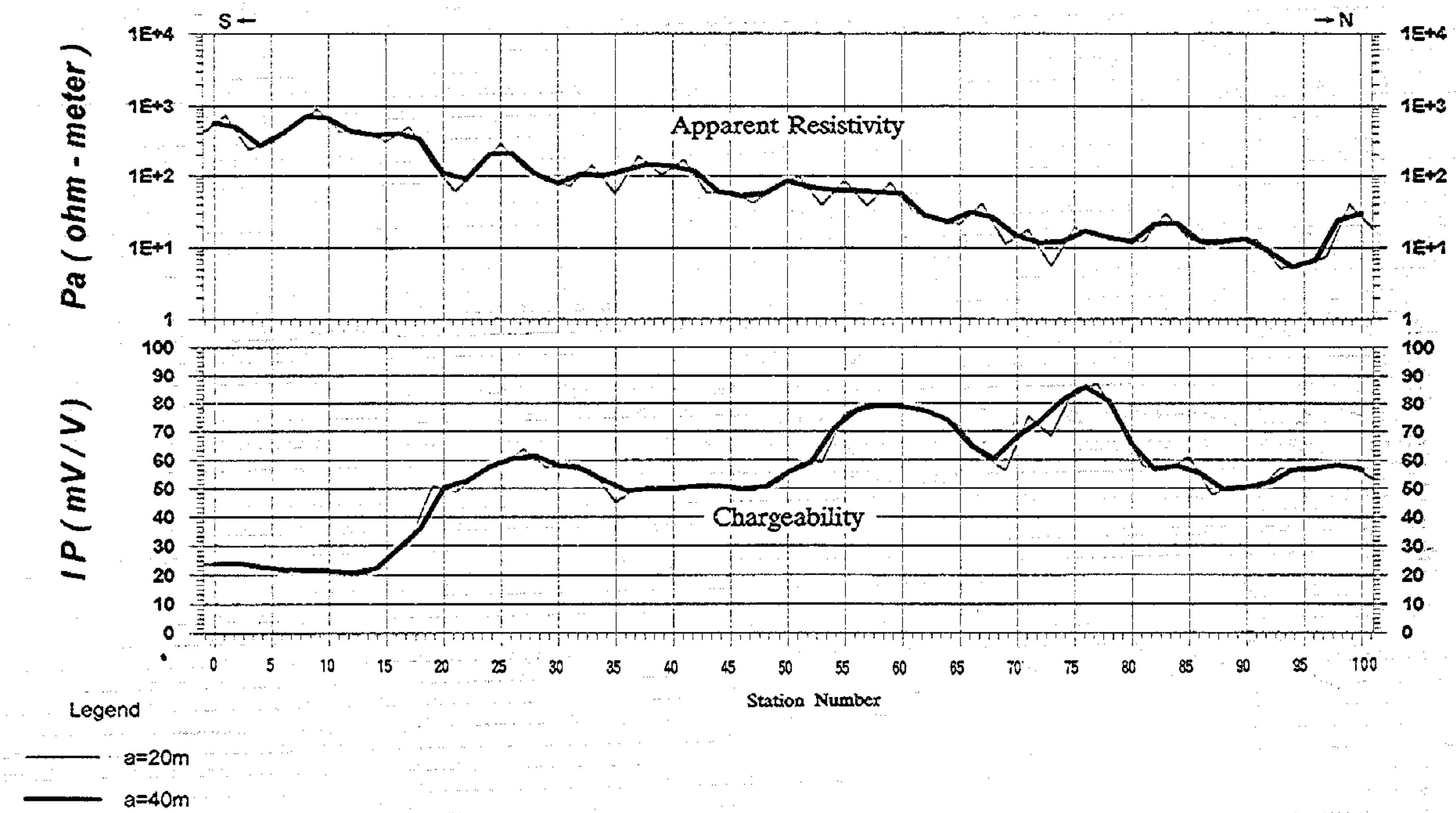

Fig.II–3–3–4(3) Apparent Resistivity and Chargeability Section (TDIP Line–3)

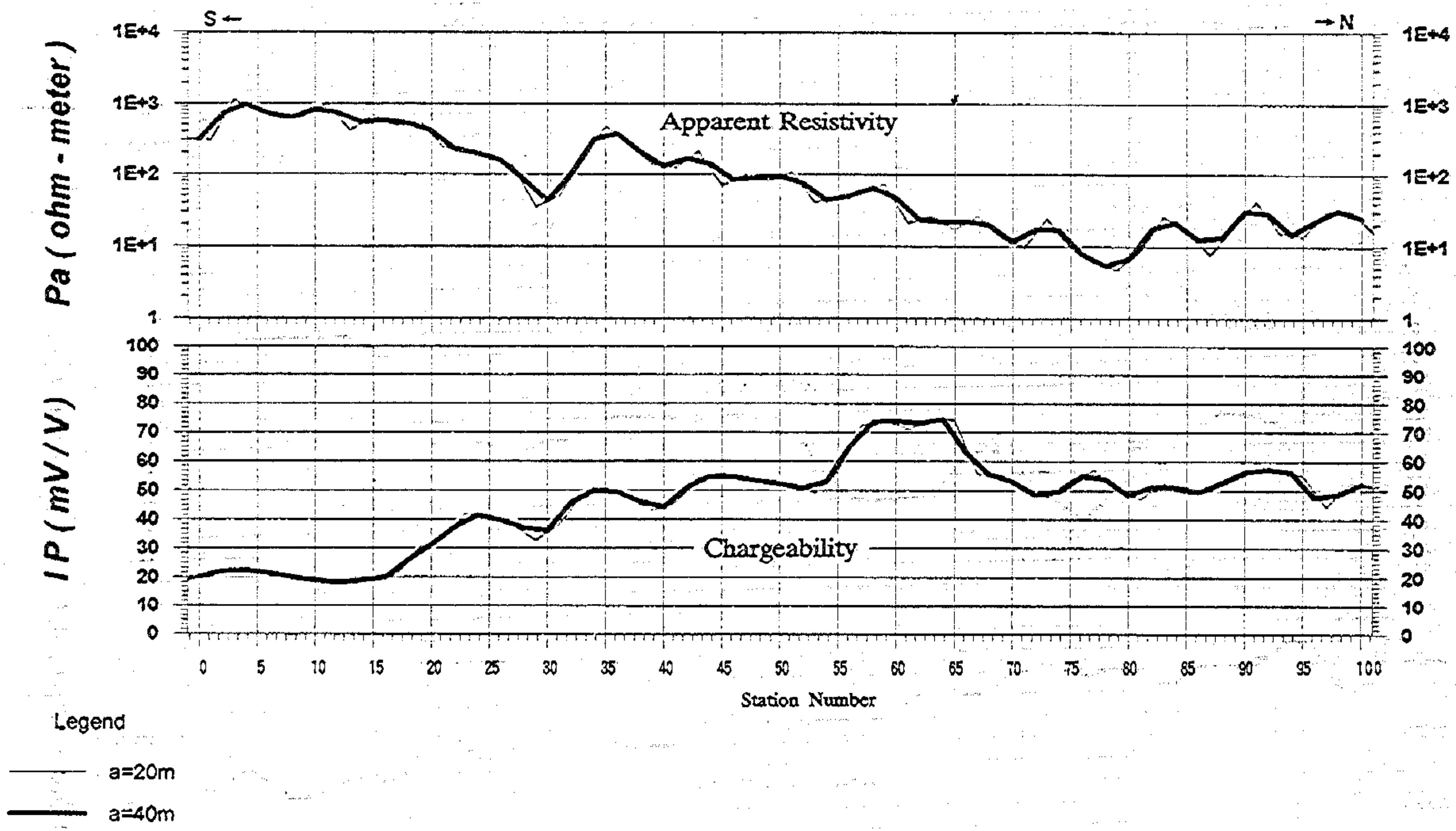

Fig.II–3–3–4(4) Apparent Resistivity and Chargeability Section (TDIP Line–4)

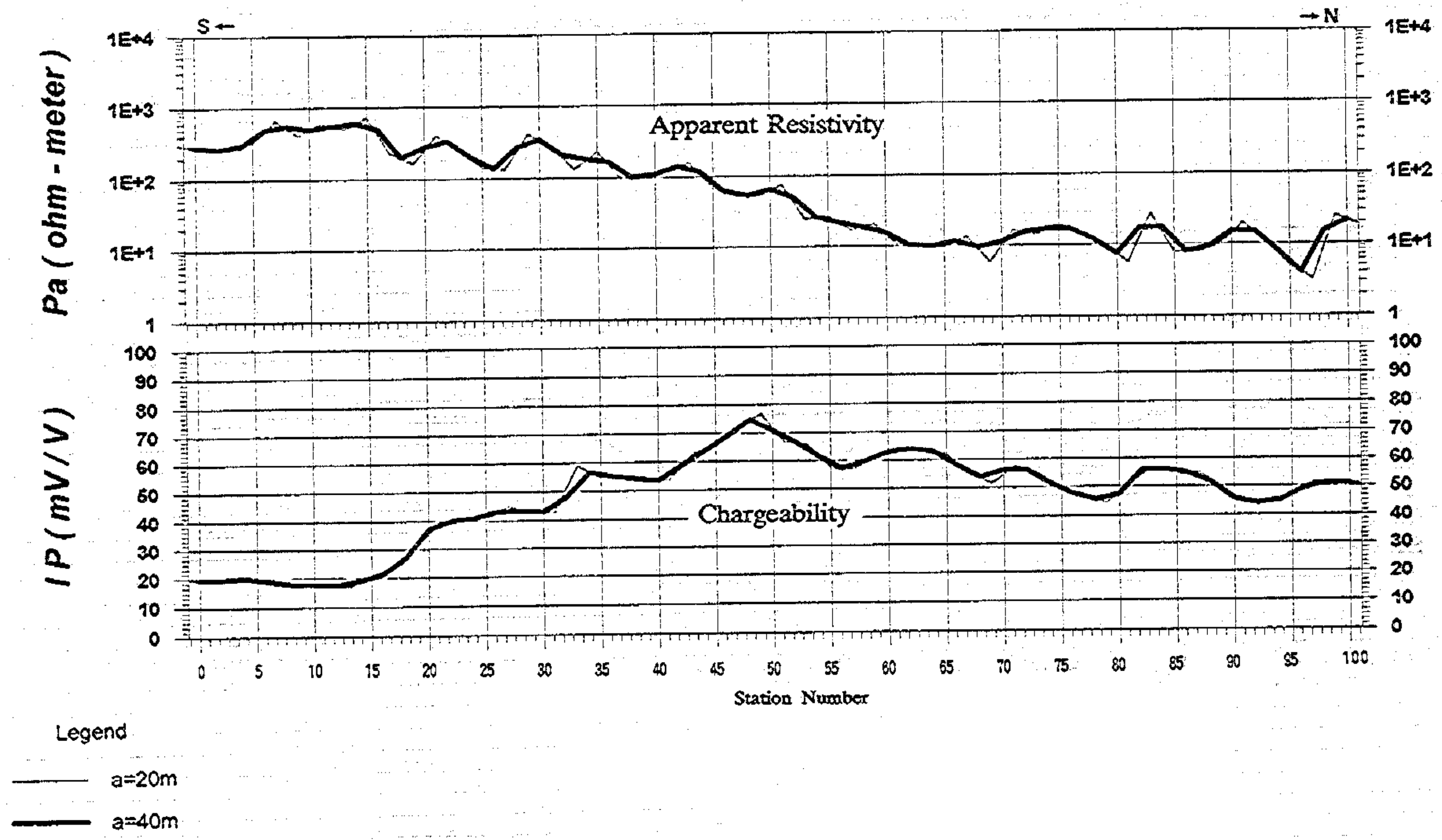

Fig.II–3–3–4(5) Apparent Resistivity and Chargeability Section (TDIP Line–5)

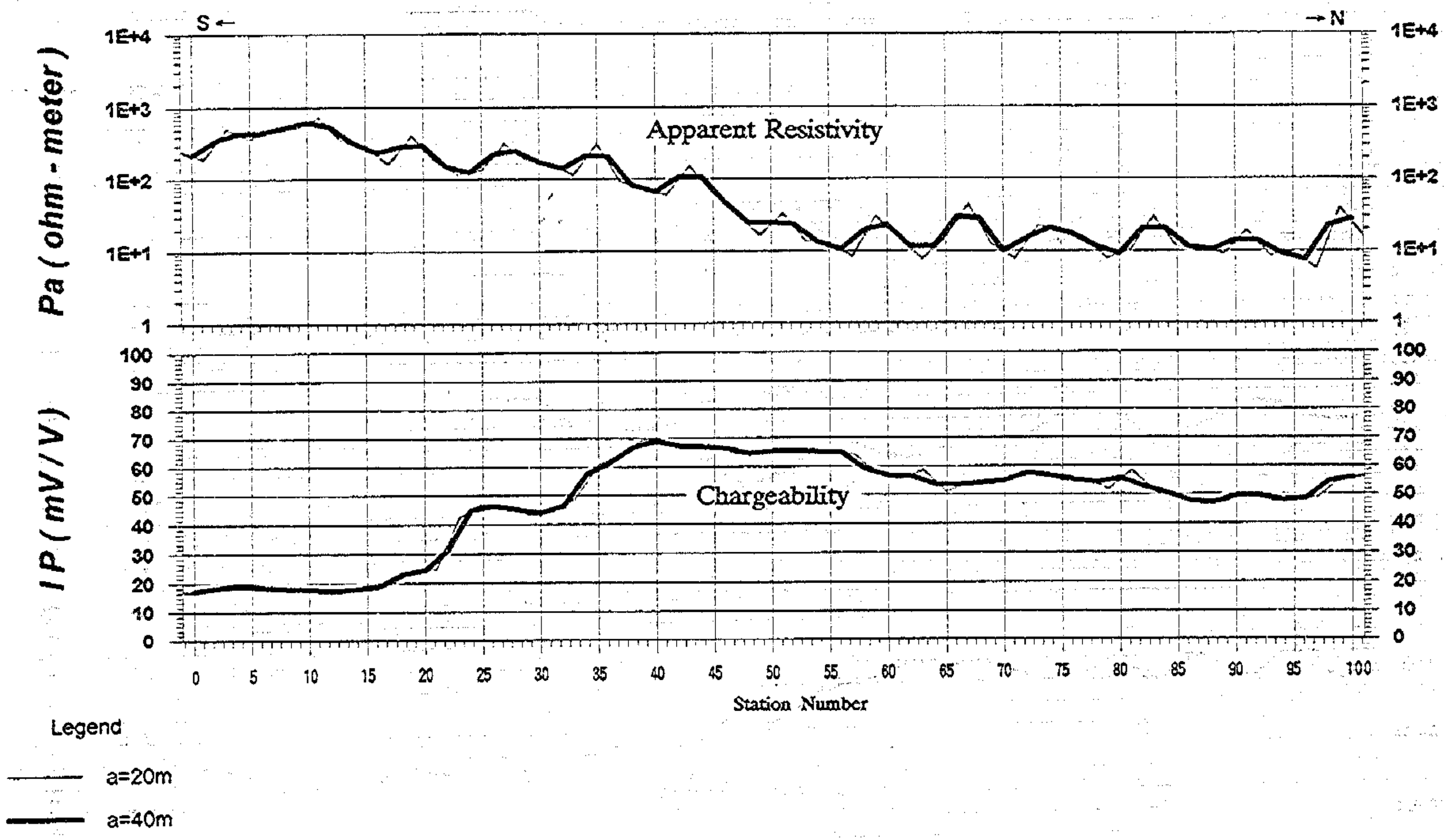

Fig.II–3–3–4(6) Apparent Resistivity and Chargeability Section (TDIP Line–6)

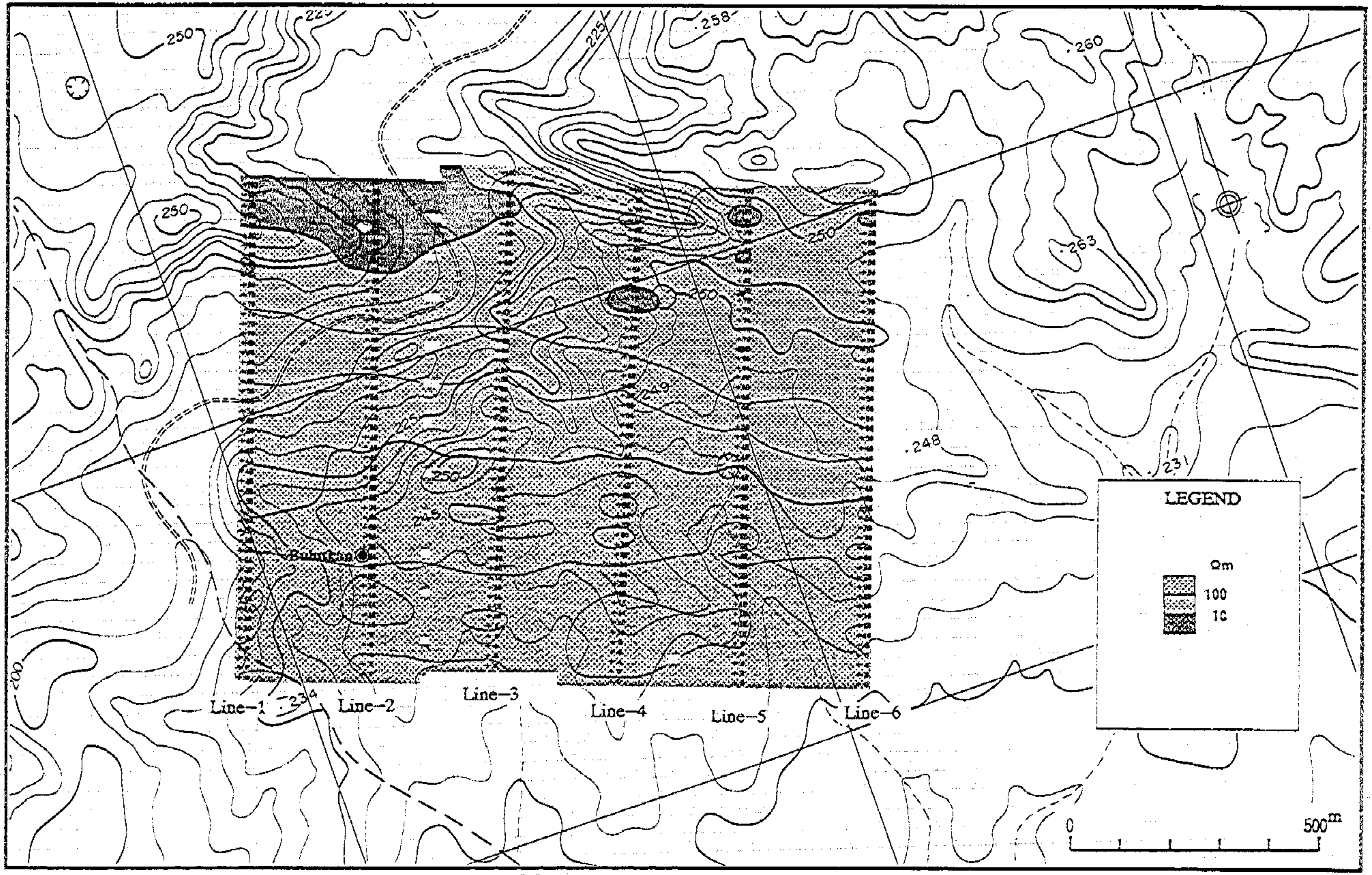

Fig.II–3–3–5 Apparent Resistivity Map

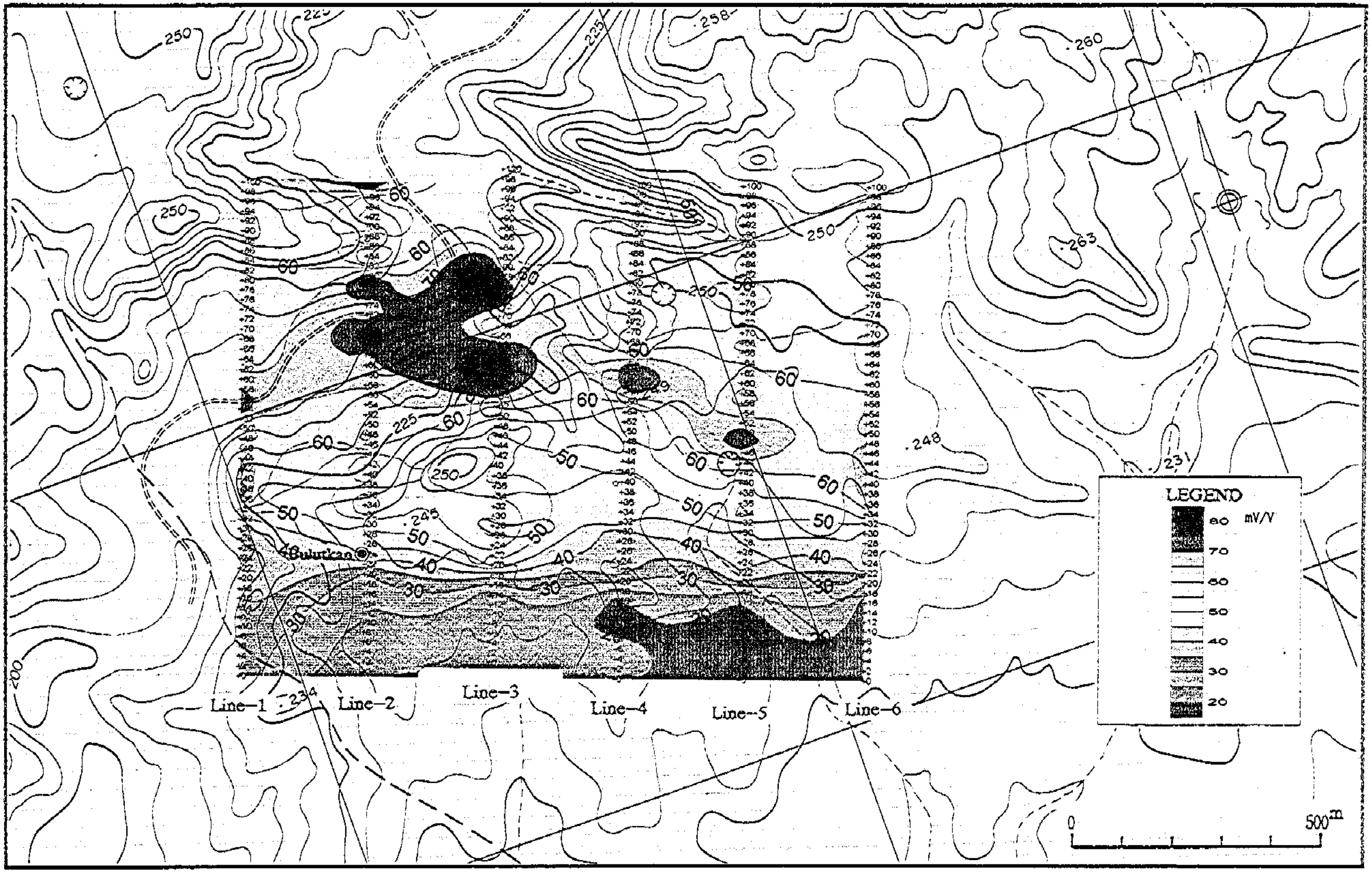

Fig.II-3-3-6 Chargeability Distribution Map

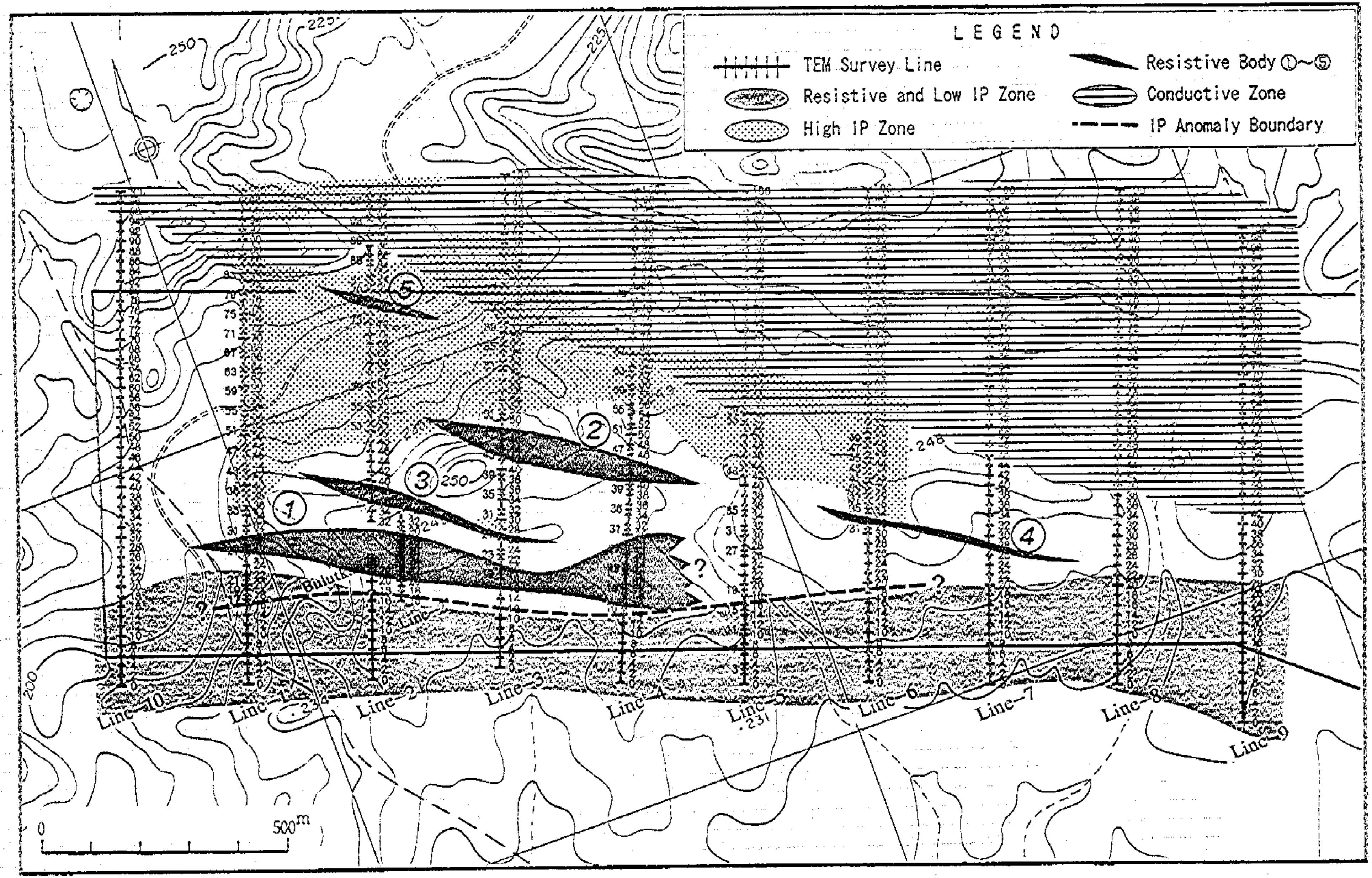

Fig.II-3-3-7 Geophysical Interpretation Map

Table II-3-3-1 Resistivity Summary

	"Southern Structure" Area	"Central Structure" Area	"Northern Structure" Area
Line-1	① Area: No. 0 to 24. ② The boundary between "Southern Structure" and "Central Structure" dips northward at a depth. ③ Dike shaped resistive bodies are at a depth between No. 0 and No. 4 and between No. 14 and No. 17.	① Area: No.26 to 80. ② A resistive body is between No.26 and 30, near the boundary to "Southern Structure", at near the surface	① Area: No. 82 to 100.
Line-2	① Area: No. 0 to 16. ② A resistive to very resistive body is between No. 0 and No. 10 at 50 m and 200 m above sea level.	① Area: No. 18 to 88. ② A resistivity structure in this area is very complex. ③ A resistive to very resistive body continues from a surface to a depth between No. 19 and No. 31 where is at Bulutkan ore deposit. ④ A resistive body is between No. 36 and No. 40 at 50 m and 150 m above sea level. ⑤ Very conductive bodies are around a resistive body is between No. 76 and No. 79 at 100 m and 150 m above sea level.	① Area: No. 89 to 100. ② Dike shaped medium resistivity body is between No.94 to No. 96 at near the surface.
Line-3	① Area: No. 0 to 12. ② A resistive to very resistive body is between No. 0 and No. 8 at 100 m and 200 m above sea level.	① Area: No. 14 to 66. ② A resistive to very resistive body is between No. 16 and No. 20 at near the surface. ③ Resistive bodies are between No. 26 to No. 27 at 80 m and 100 m and between No. 42 to No. 50 at 140 m and 220 m above sea level.	① Area: No. 68 to 100.
Line-4	① Area: No. 0 to 14. ② Structure is horizontally layered. The boundary between "Southern Structure" and "Central Structure" dips northward.	① Area: No. 15 to 64. ② A very conductive body is under a resistive to very resistive body that continues from a surface to 120 m above sea level between No. 15 to No. 30 ③ A resistive body is between No. 39 to No. 46 at near the surface.	① Area: No. 66 to 100. ② A very conductive body is between No.92 to No.100 at a depth.
Line-5	① Area: No 0 to 20. ② The boundary between "Southern Structure" and "Central Structure" dips southward. ③ A resistive body is between No. 0 and No. 6 at 100 m and 200 m above sea level.	① Area: No. 22 to 55.	① Area: No. 56 to 100.
Line-6	① Area: No. 0 to 18 ② The boundary between "Southern Structure" and "Central Structure" dips southward. ③ Resistive bodies are between No. 0 and No. 6 at 100 m and 200 m above sea level and between No. 18 and No. 19 at the near the surface.	① Area: No. 20 to 52. ② A resistive body is between No. 32 to No. 34 at near the surface.	① Area: No. 54 to 100.
Line-7	① Area: No. 0 to 20. ② Small resistive to very resistive bodies are at near the surface.	① Area: No. 22 to 46. ② A resistive body is at No. 28.	① Area: No. 48 to 100. ② A very conductive layer continues to a depth between No. 72 to No.82.
Line-8	① Area: No. 0 to 20. ② Small resistive to very resistive bodies are at near the surface.	① Area: No. 24 to 38.	① Area: No. 40 to 100. ② A very conductive layer continues to a depth between No. 64 to No 86.
Line-9	① Area: No. 0 to 28(?). ② A large resistive to very resistive body continues to a depth.	① Area: No. 30(?) to 42. ② A medium resistivity layer is at near the surface.	① Area: No. 44 to 100. ② Small medium resistivity to resistive bodies are at near the surface.
Line-10	① Area: No. 0 to 18. ② A medium resistivity layer is between resistive layers at 100 m above sea level.	① Area: No. 20 to 94. ② A resistivity structure in this zone is very complex. ③ A medium resistivity to resistive body continues from the surface to sea level between No. 20 to No. 56. ④ Very conductive body is between No 70 to No. 88 at 190 m above sea level	① Area: No. 96 to 100.

Table II-3-3-2 Apparent Resistivity and Chargeability

(1/6)

line-1 No.	a=20m IP (mV/V)	a=40m ρa (Ωm)	a=20m IP (mV/V)	a=40m ρa (Ωm)	line-1 No.	a=20m IP (mV/V)	a=40m ρa (Ωm)	a=20m IP (mV/V)	a=40m ρa (Ωm)
-1	40.3	65			51	56.8	41		
0			33.8	79	52			67.4	47
1	29.1	92			53	75.5	53		
2			32.9	613	54			76.0	48
3	33.2	1145			55	76.6	43		
4			34.1	863	56			72.6	78
5	35.8	573			57	71.1	112		
6			34.9	493	58			68.7	84
7	33.5	410			59	64.0	57		
8			34.2	548	60			66.7	45
9	34.6	692			61	71.4	33		
10			33.2	839	62			68.0	27
11	32.2	992			63	63.1	22		
12			32.2	830	64			59.7	36
13	32.3	661			65	58.3	50		
14			33.7	601	66			56.6	38
15	35.4	538			67	53.5	26		
16			35.5	384	68			56.5	28
17	35.8	224			69	58.9	30		
18			44.6	511	70			61.5	30
19	47.1	809			71	64.2	29		
20			46.0	585	72			61.6	31
21	43.5	351			73	59.5	34		
22			40.4	343	74			60.3	23
23	36.9	335			75	62.0	13		
24			34.2	268	76			62.7	12
25	29.5	199			77	63.5	11		
26			28.1	198	78			61.7	14
27	26.6	198			79	60.5	16		
28			27.8	141	80			61.7	14
29	30.6	82			81	63.4	12		
30			34.2	92	82			63.4	9
31	37.1	102			83	63.4	5		
32			38.2	104	84			62.6	5
33	39.4	106			85	61.8	5		
34			50.6	99	86			58.6	13
35	63.8	93			87	57.8	21		
36			68.9	75	88			55.6	25
37	77.4	56			89	54.2	30		
38			75.6	45	90			53.6	22
39	72.6	33			91	52.6	15		
40			70.7	45	92			53.3	8
41	69.5	57			93	63.4	1		
42			71.5	43	94			59.4	3
43	75.5	29			95	58.6	4		
44			70.6	37	96			53.8	3
45	67.5	46			97	42.6	2		
46			61.9	43	98			59.5	6
47	55.5	41			99	62.8	9		
48			51.7	83	100			63.4	8
49	50.5	126			101	64.3	6		
50			52.0	83					

line-2 No.	a=20m IP (mV/V)	a=40m ρa (Ωm)	a=20m IP (mV/V)	a=40m ρa (Ωm)	line-2 No.	a=20m IP (mV/V)	a=40m ρa (Ωm)	a=20m IP (mV/V)	a=40m ρa (Ωm)
-1	19.5	428			51	64.0	122		
0			22.2	519	52			64.4	91
1	24.3	630			53	65.2	59		
2			23.7	793	54			63.5	53
3	23.2	987			55	61.4	47		
4			23.0	588	56			62.0	58
5	20.5	119			57	62.5	70		
6			23.2	203	58			66.1	74
7	24.5	300			59	69.4	78		
8			24.4	278	60			69.2	58
9	24.3	252			61	68.8	38		
10			25.0	561	62			68.4	40
11	25.2	910			63	68.0	41		
12			25.1	796	64			69.6	34
13	24.9	668			65	72.0	26		
14			25.1	631	66			76.3	34
15	25.2	589			67	78.9	41		
16			25.8	580	68			77.4	29
17	26.5	571			69	74.2	18		
18			27.3	751	70			72.0	15
19	27.8	948			71	68.9	12		
20			29.8	626	72			65.7	12
21	36.9	278			73	62.6	12		
22			37.9	173	74			68.0	13
23	42.6	61			75	72.0	14		
24			45.8	89	76			74.0	11
25	47.5	119			77	77.8	7		
26			47.5	157	78			78.9	12
27	47.5	197			79	79.2	17		
28			48.4	184	80			75.8	13
29	49.4	171			81	70.3	10		
30			50.7	119	82			58.3	10
31	54.5	64			83	47.4	10		
32			62.7	123	84			45.8	8
33	65.7	185			85	43.2	6		
34			63.3	234	86			46.6	5
35	61.7	284			87	51.1	4		
36			58.3	202	88			67.1	5
37	49.7	117			89	74.5	7		
38			47.8	129	90			54.1	12
39	46.2	142			91	46.6	17		
40			45.3	128	92			47.3	13
41	44.2	114			93	48.3	10		
42			44.2	149	94			49.8	7
43	44.3	185			95	52.6	5		
44			48.1	130	96			51.1	3
45	57.8	74			97	46.9	1		
46			62.2	73	98			71.8	3
47	66.8	72			99	77.2	5		
48			66.4	83	100			76.2	3
49	66.2	94			101	73.8	2		
50			64.9	108					

line-3 No.	a=20m IP (mV/V)	a=40m ρa (Ωm)	a=20m IP (mV/V)	a=40m ρa (Ωm)
-1	23.5	415		
0			23.9	574
1	24.2	735		
2			24.1	491
3	23.8	241		
4			22.8	268
5	21.8	296		
6			21.9	410
7	22.0	527		
8			21.6	713
9	21.4	905		
10			21.4	669
11	21.5	423		
12			20.8	431
13	20.0	439		
14			22.1	376
15	25.1	311		
16			29.0	404
17	31.5	501		
18			36.0	331
19	50.9	154		
20			50.3	108
21	48.8	60		
22			52.7	91
23	54.8	123		
24			57.6	203
25	58.9	286		
26			60.4	209
27	63.8	129		
28			61.3	107
29	57.2	85		
30			58.1	79
31	59.2	72		
32			57.0	106
33	55.8	141		
34			52.8	99
35	45.1	57		
36			49.1	123
37	50.3	190		
38			49.9	146
39	49.1	102		
40			49.8	136
41	50.3	169		
42			50.7	114
43	51.8	57		
44			50.9	59
45	50.0	62		
46			49.7	52
47	49.2	42		
48			50.5	57
49	51.2	71		
50			55.6	85

line-3 No.	a=20m IP (mV/V)	a=40m ρa (Ωm)	a=20m IP (mV/V)	a=40m ρa (Ωm)
51	58.8	98		
52			58.9	69
53	59.2	39		
54			70.8	63
55	76.2	86		
56			77.3	62
57	79.7	38		
58			79.2	59
59	78.9	80		
60			78.7	55
61	78.3	32		
62			77.1	28
63	75.7	25		
64			73.8	23
65	71.7	21		
66			64.8	31
67	61.4	41		
68			60.3	26
69	56.3	11		
70			68.0	15
71	75.2	18		
72			73.5	12
73	68.3	6		
74			81.4	12
75	85.2	19		
76			85.9	17
77	86.8	15		
78			80.8	14
79	73.5	12		
80			65.6	12
81	58.0	12		
82			56.8	21
83	56.3	30		
84			57.8	22
85	61.1	14		
86			55.1	12
87	47.8	11		
88			49.6	12
89	50.9	14		
90			50.4	13
91	49.8	13		
92			52.0	9
93	57.1	5		
94			56.6	5
95	56.2	6		
96			57.0	7
97	57.5	8		
98			58.2	24
99	58.3	40		
100			56.7	29
101	53.4	19		

line-4 No.	a=20m IP (mV/V)	a=40m ρa (Ωm)	a=20m IP (mV/V)	a=40m ρa (Ωm)
-1	18.9	315		
0			20.0	307
1	21.2	298		
2			22.0	706
3	22.2	1123		
4			22.2	959
5	22.2	791		
6			21.3	701
7	20.2	608		
8			19.9	624
9	19.7	640		
10			18.8	823
11	18.2	1014		
12			18.1	717
13	18.0	408		
14			18.7	536
15	19.1	670		
16			19.8	574
17	20.9	474		
18			25.8	515
19	30.2	558		
20			31.0	401
21	33.1	237		
22			37.2	224
23	42.0	210		
24			41.4	196
25	40.8	181		
26			39.7	157
27	38.2	131		
28			37.0	83
29	32.6	34		
30			35.9	42
31	38.2	50		
32			45.7	100
33	48.3	151		
34			49.9	307
35	50.5	467		
36			49.4	370
37	47.5	271		
38			46.1	205
39	43.1	138		
40			44.3	130
41	45.7	121		
42			51.1	164
43	54.3	208		
44			54.7	139
45	56.0	69		
46			54.6	83
47	53.5	97		
48			53.3	89
49	53.1	80		
50			52.1	94

line-4 No.	a=20m IP (mV/V)	a=40m ρa (Ωm)	a=20m IP (mV/V)	a=40m ρa (Ωm)
51	51.4	107		
52			50.8	74
53	49.4	41		
54			53.1	43
55	56.5	45		
56			65.0	50
57	72.0	55		
58			73.4	64
59	74.5	72		
60			73.7	46
61	70.9	21		
62			72.9	23
63	74.5	26		
64			74.3	21
65	74.2	17		
66			62.9	21
67	55.7	26		
68			55.5	20
69	55.1	13		
70			53.0	12
71	50.3	10		
72			48.6	17
73	48.0	24		
74			49.6	17
75	53.5	10		
76			54.8	8
77	56.8	6		
78			53.9	5
79	50.3	5		
80			48.3	7
81	47.2	9		
82			51.3	17
83	52.6	26		
84			51.2	21
85	49.2	17		
86			49.5	12
87	50.2	8		
88			52.7	13
89	53.7	19		
90			56.3	30
91	57.4	41		
92			57.3	28
93	57.2	15		
94			56.1	15
95	54.8	14		
96			47.6	22
97	44.5	30		
98			48.6	31
99	52.5	32		
100			52.1	24
101	51.5	16		

line-5 No.	a=20m IP (mV/V)	a=40m ρa (Ωm)	a=20m IP (mV/V)	a=40m ρa (Ωm)
-1	19.7	298		
0			19.4	281
1	19.1	261		
2			19.5	264
3	20.0	268		
4			20.0	299
5	20.0	335		
6			18.7	488
7	18.0	664		
8			17.9	547
9	17.8	412		
10			17.8	499
11	17.8	597		
12			17.4	550
13	16.8	497		
14			18.9	602
15	20.6	718		
16			21.3	487
17	23.7	233		
18			26.9	200
19	31.8	164		
20			37.1	278
21	39.4	403		
22			40.0	331
23	40.9	254		
24			41.0	201
25	41.2	143		
26			43.0	139
27	44.9	135		
28			43.4	267
29	42.9	407		
30			43.0	346
31	43.1	283		
32			47.9	209
33	58.8	133		
34			56.4	181
35	54.9	232		
36			55.0	167
37	55.2	100		
38			54.1	101
39	52.9	101		
40			53.4	112
41	53.8	123		
42			58.7	140
43	62.6	158		
44			63.7	114
45	66.2	70		
46			69.0	62
47	72.6	54		
48			74.6	53
49	76.6	53		
50			70.8	64

line-5 No.	a=20m IP (mV/V)	a=40m ρa (Ωm)	a=20m IP (mV/V)	a=40m ρa (Ωm)
51	66.8	75		
52			66.5	50
53	65.7	24		
54			61.4	25
55	57.4	26		
56			57.1	21
57	56.8	17		
58			59.6	18
59	61.8	20		
60			62.7	15
61	64.2	11		
62			63.8	10
63	63.4	10		
64			62.7	10
65	62.0	9		
66			57.8	11
67	54.8	13		
68			53.7	9
69	51.5	6		
70			56.0	11
71	57.5	16		
72			56.2	15
73	54.8	14		
74			51.3	17
75	48.9	19		
76			47.7	17
77	46.2	14		
78			45.5	12
79	44.6	9		
80			47.4	7
81	51.8	6		
82			55.9	17
83	56.6	27		
84			56.1	17
85	54.5	8		
86			54.6	8
87	54.8	8		
88			51.5	9
89	49.2	10		
90			45.7	15
91	44.2	19		
92			44.1	15
93	44.0	11		
94			45.1	8
95	47.2	5		
96			49.0	4
97	51.4	3		
98			51.1	15
99	51.1	24		
100			50.8	21
101	50.5	18		

line-6 No.	a=20m IP (mV/V)	a=40m ρa (Ωm)	a=20m IP (mV/V)	a=40m ρa (Ωm)
-1	16.8	250		
0			17.1	222
1	17.5	193		
2			18.3	353
3	18.6	515		
4			19.0	444
5	19.5	371		
6			18.4	449
7	17.5	529		
8			18.1	529
9	18.6	529		
10			17.7	630
11	17.1	736		
12			17.2	541
13	17.5	338		
14			17.9	323
15	18.3	306		
16			18.8	236
17	19.8	163		
18			22.9	286
19	24.2	415		
20			24.4	302
21	25.1	184		
22			31.6	150
23	42.5	115		
24			44.9	124
25	47.1	134		
26			46.3	224
27	46.0	317		
28			45.1	251
29	43.4	183		
30			43.9	175
31	44.5	167		
32			46.2	141
33	48.8	115		
34			57.4	216
35	60.6	320		
36			61.4	207
37	64.3	92		
38			66.7	81
39	69.8	70		
40			68.9	65
41	67.8	60		
42			67.1	106
43	66.8	152		
44			66.9	107
45	67.4	62		
46			66.3	47
47	64.3	33		
48			64.4	25
49	64.6	16		
50			65.3	25

line-6 No.	a=20m IP (mV/V)	a=40m ρa (Ωm)	a=20m IP (mV/V)	a=40m ρa (Ωm)
51	65.7	33		
52			65.4	23
53	64.8	14		
54			65.0	13
55	65.2	13		
56			64.9	11
57	64.3	8		
58			59.0	19
59	57.5	30		
60			56.7	23
61	55.2	15		
62			56.4	12
63	58.6	8		
64			53.6	11
65	51.1	15		
66			53.4	30
67	54.2	44		
68			54.0	28
69	53.7	12		
70			54.8	10
71	56.6	8		
72			57.5	15
73	57.8	22		
74			56.5	21
75	54.9	19		
76			55.1	17
77	55.4	15		
78			54.1	11
79	51.7	8		
80			55.5	9
81	58.3	10		
82			52.8	20
83	50.9	30		
84			50.3	20
85	48.8	11		
86			47.7	11
87	46.6	11		
88			46.9	10
89	47.2	9		
90			49.5	14
91	50.5	19		
92			49.5	14
93	47.5	9		
94			47.8	9
95	48.0	9		
96			48.3	7
97	48.9	6		
98			54.6	22
99	55.4	39		
100			55.7	27
101	56.3	16		

Table Ⅱ-3-3-3 Resistivity and Chargeability of Rock Samples

Sample No.	Locality			Rock name	Py	Resistivity (ohm-m)	I P (mV/V)
B-1B1	MJUB-1	37.5	m	Metasomatite	○	357	380.7
B-1B2	MJUB-1	44.4	m	Metasomatite	○	17,073	20.8
B-1B3	MJUB-1	59.5	m	Metasomatite		22,920	5.1
B-1B4	MJUB-1	77.5	m	Metasomatite		74,964	8.2
B-1B5	MJUB-1	85.5	m	Skarn	○	1,245	20.1
B-1B6	MJUB-1	149.6	m	Syenodiorite		802	1.6
B-2B1	MJUB-2	11.4	m	Limy sandstone		123,271	19.1
B-2B2	MJUB-2	17.6	m	Limestone		35,569	7.2
B-2B3	MJUB-2	35.8	m	Metasomatite	○	757	26.5
B-2B4	MJUB-2	95.1	m	Sulphide vein	○	0.9	181.6
B-2B5	MJUB-2	99.8	m	Alt. (ss>sl)	○	2,149	143.3
B-2B6	MJUB-2	109.2	m	Metasomatite	○	278	344.1
B-2B7	MJUB-2	189.5	m	Syenodiorite		9,248	3.1
B-3B1	MJUB-3	24.3	m	Skarnized sandstone	○	21	32.3
B-3B2	MJUB-3	45.3	m	Hornfels(ss)	○	17	119.0
B-3B3	MJUB-3	50.0	m	Alt. (sl>ss)	○	24	230.2
B-3B4	MJUB-3	64.0	m	Limestone		18,392	7.8
B-3B5	MJUB-3	81.5	m	Sulphide vein	○	0.4	288.4
B-3B6	MJUB-3	96.0	m	Marble with wollastonite		2,836	4.3
B-3B7	MJUB-4	130.6	m	Syenodiorite		302	3.2
B-4B1	MJUB-4	20.8	m	Granite		74	13.2
B-4B2	MJUB-4	22.4	m	Limestone		5,566	5.0
B-4B3	MJUB-4	45.9	m	Metasomatite	○	1,372	118.4
B-4B4	MJUB-4	64.0	m	Sandstone		45,393	22.2
B-4B5	MJUB-4	85.5	m	Lamprophyre	○	742	134.3
B-4B6	MJUB-4	103.8	m	Syenodiorite		46,400	8.5
B-6B1	MJUB-6	35.4	m	Alt. (sl>ss)	○	2,491	31.0
B-6B2	MJUB-6	48.0	m	Metasomatite	○	43	128.5
B-6B3	MJUB-6	78.5	m	Porohyrite		6,766	17.3
B-6B4	MJUB-6	82.7	m	Alt. (sl>ss)	○	44,041	187.7
B-6B5	MJUB-6	133.7	m	Alt. (sl>ss)	○	96,593	5.2
B-7B1	MJUB-7	9.4	m	Chalcedony		166	1.3
B-7B2	MJUB-7	24.3	m	Lamprophyre		13	8.1
B-7B3	MJUB-7	49.4	m	Skarn	○	6.7	133.0
B-7B4	MJUB-7	59.4	m	Metasomatite		4,101	22.4
B-7B5	MJUB-7	71.8	m	Diorite		2,739	23.1
B-5B1	MJUB-5	6.8	m	Dolomite		29	2.0
B-5B2	MJUB-5	36.0	m	Lamprophyre		580	6.7
B-5B3	MJUB-5	100.2	m	Limestone		5,989	3.7
B-5B4	MJUB-5	106.6	m	Diorite		65,087	6.4

Rock type	Resistivity (ohm-m)	I P (mV/V)
Syenodiorite	14,200	4
Sulphide vein	1	240
Altered rock	9,000	89
No altered rock	29,200	60
Others	10,900	30
average	16,000	68

remark:Alt.=Alternation of strata,sl=slate,ss=sandstone

3-4 Drilling Survey

3-4-1 Purpose of survey

It was planned to conduct drilling survey on the following areas to examine mineralization in the deep part.

① Bulutkan gold deposit accompanying the silicified veins.

② Ore showings confirmed by this year's trenching survey.

③ The area where occurrence of gold mineralization zones is presumable from the resistivity structure and IP values found out by this year's geophysical survey.

3-4-2 Methods of survey

1) Drilling work at seven drillholes totaling 1,011.0m was carried out with personnel and equipment arranged by the Samarkand Geology. For the supervision of the work, a drilling engineer was sent from Japan.

Locations of the respective boreholes are shown in Figs. II-3-1-1 and II-3-2-1.

Two drilling machines -- the Russian-made SKB-5P (drilling cap. ϕ76m : 600-650m ; ϕ59m : 800m) were used.

The drilling work was performed in two 12-hour shifts, with one foreman and one worker per unit in principle.

Buldozers were used for the transportation of drilling machines and supplies, road construction, leveling of the drilling sites and preparatory work.

For the drilling operation, the conventional method was applied. In an effort to improve core recovery and work progress, ejectors were used together with core tubes.

The surface soil portion was drilled with single diamond bits and metal bits while, after reaching the rock, casing pipes, ϕ108mm and ϕ89mm, were inserted and installed, and thereafter, drilling was advanced with ϕ76mm or ϕ59mm diamond bits as the final diameters. Mud water prepration was not done at the drilling site but at the mud water plant of the Kokpatas Expedition base and conveyed to the site by a 8m^3 tank truck.

The drilling work lasted for 150 days from July 19 thru December 15, 1995. The drilling length and core recovery are shown in Table II-3-4-1 below:

Table II -3-4-1 Quantity of Drilling Works and Core Recovery in the Bulutkan District

Hole No.	Programmed length (m)	Length (m)	Length of Core (m)	Core recovery (%)
MJUB-1	150	150.0	120.4	80.3
MJUB-2	200	200.0	181.15	90.6
MJUB-3	140	143.5	120.7	84.1
MJUB-4	130	130.0	107.9	83.0
MJUB-5	134	134.0	108.9	81.3
MJUB-6	130	153.0	129.8	84.8
MJUB-7	100	100.5	82.3	81.9
Total	984	1,011.0	851.15	84.2

The drilling efficiency, working time, consumption of drilling articles and diamond bits are shown in Tables II-3-4-2 thru II-3-4-5, respectively. The main equipments used, results of the works and progress record are listed in Appendix 3-1 thru Appendix 3-3.

The Table II-3-4-6 below outlines the drilling operation.

Table II -3-4-6 Results of Drilling Works in the Bulutkan District

Hole No.		MJUB-1	MJUB-2	MJUB-3	MJUB-4	MJUB-5	MJUB-6	MJUB-7
Direction Dip		S16° W -75°	S16° W -75°	S35° W -75°	S30° W -75°	S5° W -75°	S20° W -80°	S16° W -80°
Bit	φ112mm	—	—	—	—	—	—	—
	φ 76mm	143.1m	200.0m	95.4m	130.0m	92.6m	23.0m	9.0m
	φ 59mm	6.9m	—	48.1m	—	41.4m	130.0m	91.5m
Casing	φ108mm	7.0m	15.0m	9.0m	19.0m	12.0m	9.0m	7.0m
	φ 89mm	31.0m	67.0m	24.0m	31.0m	26.0m	34.0m	31.0m
	φ 73mm	—	—	—	—	—	—	—

3-4-3 Results of survey

The drilling survey resulted in capturing of a prominent gold-bearing silicified vein and a gold-bearing skarn ore body, at the MJUB-7, one of the three boreholes aimed at the lower part of the Bulutkan ore body (the other two being MJUB-1 and -2). At the MJUB-1, too, a gold mineralization zone was encountered, though low in grade. At the MJUB-3 which was aimed at the lower side of the gold indication confirmed at the trench T-4, a low-grade mineralization was observed. The other drilling failed to capture mineralized zones of gold grade in excess of 1.0g/t. The results of the survey are shown in the grological cross sections along the drillholes (Figs. II-3-4-1 thru 5).

1) MJUB-1 : (Direction S 16° W ; inclination -75° ; drilling length 150.0m)

The drilling was aimed to clarify mineralization of the ore body of Bulutkan deposit from the surface to the depth of approximately 100m.

(1) Geology

Except the near-surface portion, the drillhole is composed of sandstone, slate and limestone of the Kokpatas Formation, as well as those metamorphosed from these rocks, such as hornfels, silicified rocks, silicified-skarnized metasomatite and skarn.

At the depth of 100.8m, the drilling entered syenodiorite body at the footwall of the deposit. Lamprophyre dikes intrude into these rocks.

(2) Mineralization

As shown in Fig. II-3-4-1, gold mineralization accompanied by silicified-skarnized metasomatite and skarn was found in the area under the known ore body. Indications of the mineralization are shown in Table II-3-4-7.

2) MJUB-2 : (Direction S16° W ; inclination -75° ; drilling length 200.0m)

The drilling was aimed to examine mineralization of the ore body from the surface to the depth of about 150m.

(1) Geology

Except the near-surface portion, the drillhole consists mainly of sandstone, slate and limestone of the Kokpatas Formation, as well as those metamorphosed from these rocks, such as hornfels, silicified rocks, silicified-skarnized metasomatite and skarn. At the depth of 113.5m, the drilling entered syenodiorite body at the footwall of the deposit. Lamprophyre dikes intrude into these rocks.

(2) Mineralization

As shown in Fig. II-3-4-1, mineralization with gold grade of 0.2g/t or higher was not found.

3) MJUB-3 : (Direction: S35° W ; inclination -75° ; drilling length 143.5m)

The drilling was intended to explore an eastern extension of the mineralization(8m in width; Au 31.0g/t) confirmed by the Kokpatas Expedition at the trench P-822, near the west side of the southern tip of the trench T-5, and also the high resistivity structure and IP anomalies confirmed by the geophysical survey at the hanging wall side of the syenodiorite.

(1) Geology

Except the near-surface portion, the borehole consists of slate, sandstone, quartzite and limestone of the Kokpatas Formation, as well as those metamorphosed from these rocks, such as hornfels, silicified-skarnized metasomatite and skarn. At the depth of 98.0m, the drilling entered syenodiorite body at the footwall of the deposit. Lamprophyre dikes intrude into these rocks.

(2) Mineralization

As shown in Fig. II-3-4-2, low grade gold mineralization accompanied by skarnized limestone was captured. Indications of mineralization are shown in Table II-3-4-7.

4) MJUB-4 : (Direction S30° W ; inclination -75° ; drilling length 130.0m)

The drilling was aimed to explore the lower part of the silicified zone (3.0m in width; Au 0.4g/t and Ag 0.7g/t) accompanied by brecciated, fine-grained quartz confirmed at the trench T-4 and also to examine the high resistivity structure and the IP anomalies confirmed by the geophysical survey.

(1) Geology

Except for the near-surface portion, the drillhole is composed mainly of sandstone and limestone of the Kokpatas Formation, as well as those metamorphosed from these rocks, such as silicified-skarnized metasomatite. At the depth of 86.3m, the drilling entered syenodiorite body at the footwall of the deposit. Lamprophyre and granite dikes intrude into these rocks. Between 72.6m and 75.1m, calcite veins accompanied by quartz were found.

(2) Mineralization

As shown in Fig. II-3-4-3, no indication of gold mineralization was captured.

5) MJUB-5 : (Direction S5° W ; inclination -76° ; drilling length 134.0m)

The drilling was intended to explore the anomalous zone (Au 0.09g/t or more) of the geochemical soil prospecting implemented by the Kokpatas Expedition and also the lower part of the silicified zone confirmed by the trenching survey.

(1) Geology

The drillhole, from the surface to the bottom, is composed of limestone, dolomite, slate and sandstone of the Kokpatas Formation, into which granodiorite and lamprophyre dikes intrude. Weak skarnization is recognized in a part of Kokpatas Formation rocks.

(2) Mineralization

As shown in Fig. II-3-4-4, no indication of gold mineralization was captured.

6) MJUB-6 : (Direction S20° W ; inclination -80° ; drilling length 153.0m)

The drilling was aimed at exploring the L-2 at around 770m, which was extracted as the area of high potentials of mineral occurrence, where this year's geophysical survey ascertained distribution of high resistivity and high IP.

(1) Geology

Except the river-bed sediments near the surface, the drillhole represents alteration of slate and sandstone strata of the Kokpatas Formation, a part of which is weakly silicified-skarnized. Porphyrite and diorite dikes intrude into these rocks.

(2) Mineralization

As shown in Fig. II-3-4-5, numerous quartz veins, from several centimeters to 30 cm in width, were encountered at the depth below 95m or more but no indication of gold mineralization was captured. Sandstone and slate disseminated with prominent pyrite of the Kokpatas Formation were recognized in this drillhole.

7) MJUB-7 : (Direction S16° W ; inclination -80° ; drilling length 100.5m)

The drilling was intended to examine mineralization of the central portion of the ore body of Bulutkan deposit from the surface to the depth of 80m.

(1) Geology

The Kokpatas Formation on the whole is prominently silicified-skarnized. The upper portion above the lamprophyre dike accompanied by limonite and gypsum veins between 16.6m and 36.1m, which forms the border, is composed of silicified rocks accompanied by gossan, fine-grained quartz veins and yellowish white-colored chalcedony, while the lower portion is comprised of skarn accompanied by sulfide veins, skarnized sandstone and silicified-skarnized metasomatite. Lamprophyre and diorite dikes intrude into the rocks. At the depth of 76.5m, the drilling entered syenodiorite body at the footwall of the deposit.

(2) Mineralization

As shown in Fig. II-3-4-1, prominent gold mineralization accompanying silicified rocks in the upper part and skarn in the lower part of the ore body was found.

Indications of mineralization are shown in Table II-3-4-7.

3-4-4 Conclusive summary and consideration

As the result of the drilling survey at the three drillholes of the ore body of Bulutkan deposit, gold mineralization was recognized at the MJUB-1 and -7 at the depths referred to in the preceding paragraph. On the surface portion of the Bulutkan deposit, a vein of 32m in true width was confirmed by trenching survey. The drilling of the MJUB-1 ascertained gold mineralization over about 10m (true width). The drilling and trenching survey resulted in confirming that the ore body strikes WNW-ESE and dips about 70° N.

The drilling survey revealed that the mineralization of the ore deposit further continues up to some 100m below the surface. The ore body with gold mineralization is silicified rocks accompanied by gossan, fine-grained quartz and chalcedony in the upper part whilst, in the lower part, it is a skarn ore body accompanied by sulfide veins. Ore shoots are of the WNE-ESE strike and are distributed in close relationship with lamprophyre and diorite dikes which intrude in the same direction.

Gold indications, though low-grade, have been confirmed also in the eastern and western extensions of the ore body by the non-coring drilling implemented by the Kokpatas

Expedition. These intrusive rocks and the ore body seem to be controlled by groups of fractures and strata bearing carbonate rocks. In view of the trenching survey findings that the carbonate rocks strike E-W ~ NE-SW and dip southward, the plunge of ore shoot is considered to dip toward the ESE direction.

In this year's survey, the drilling captured portions where gold grade exceeds 1g/t at the Bulutkan ore deposit and at the drillhole MJUB-3 between 82.0m and 84.0m (1.6m in true width; Au 2.3g/t and Ag 36.1g/t), the both occurring in the Proterozoic near the north side of a syenodiorite stock. The gold mineralization confirmed by the trenching survey are also distributed in the vicinity of the syenodiorite stock. It appears likely that, at the zone along the north side of the syenodiorite body extending in the WNW-ESE direction, there occur ore shoots similar to the ore body of Bulutkan.

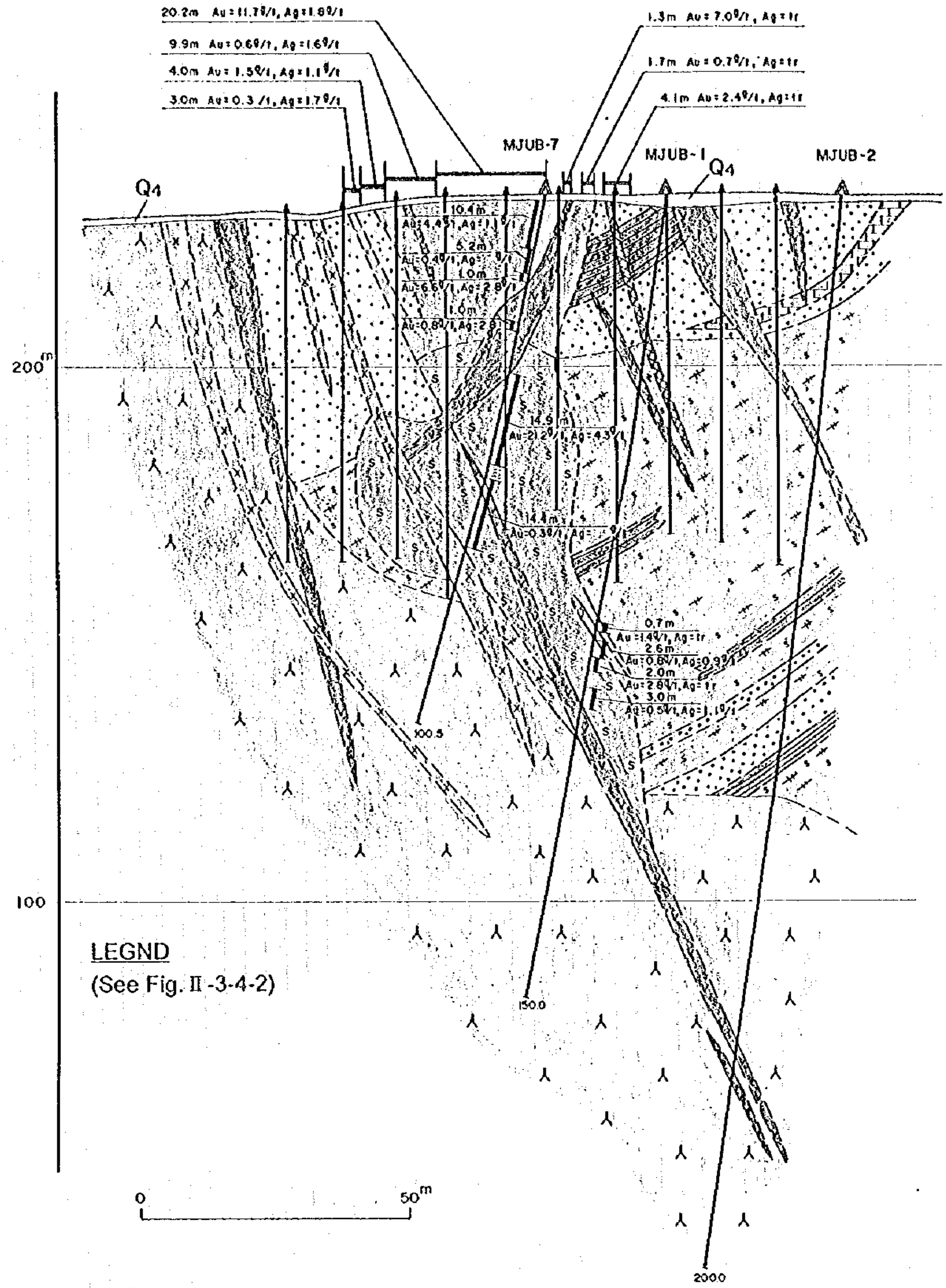

Fig. II-3-4-1 Geological Cross Section along MJUB-1,2 and 7

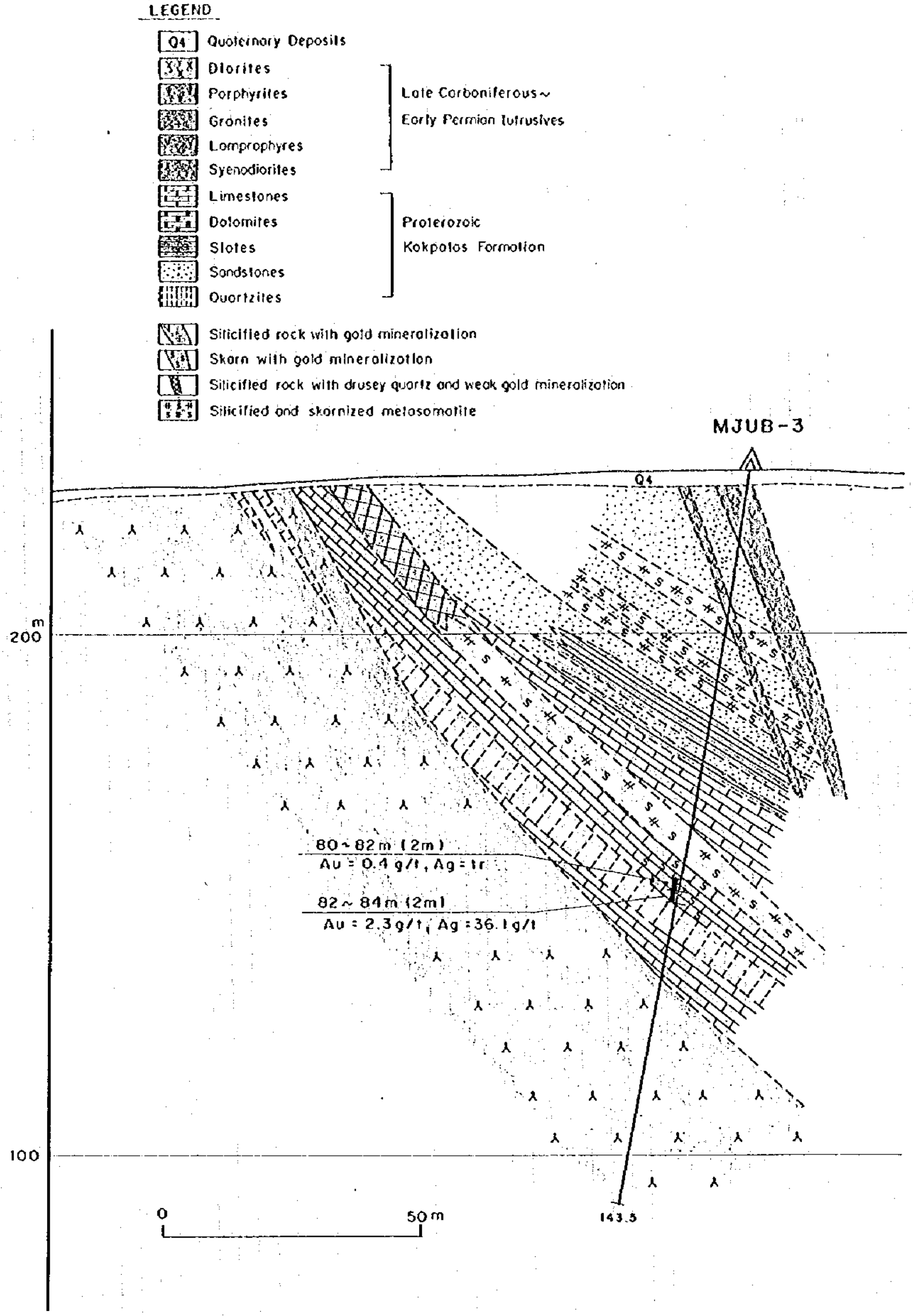

Fig. II-3-4-2 Geological Cross Section along MJUB-3

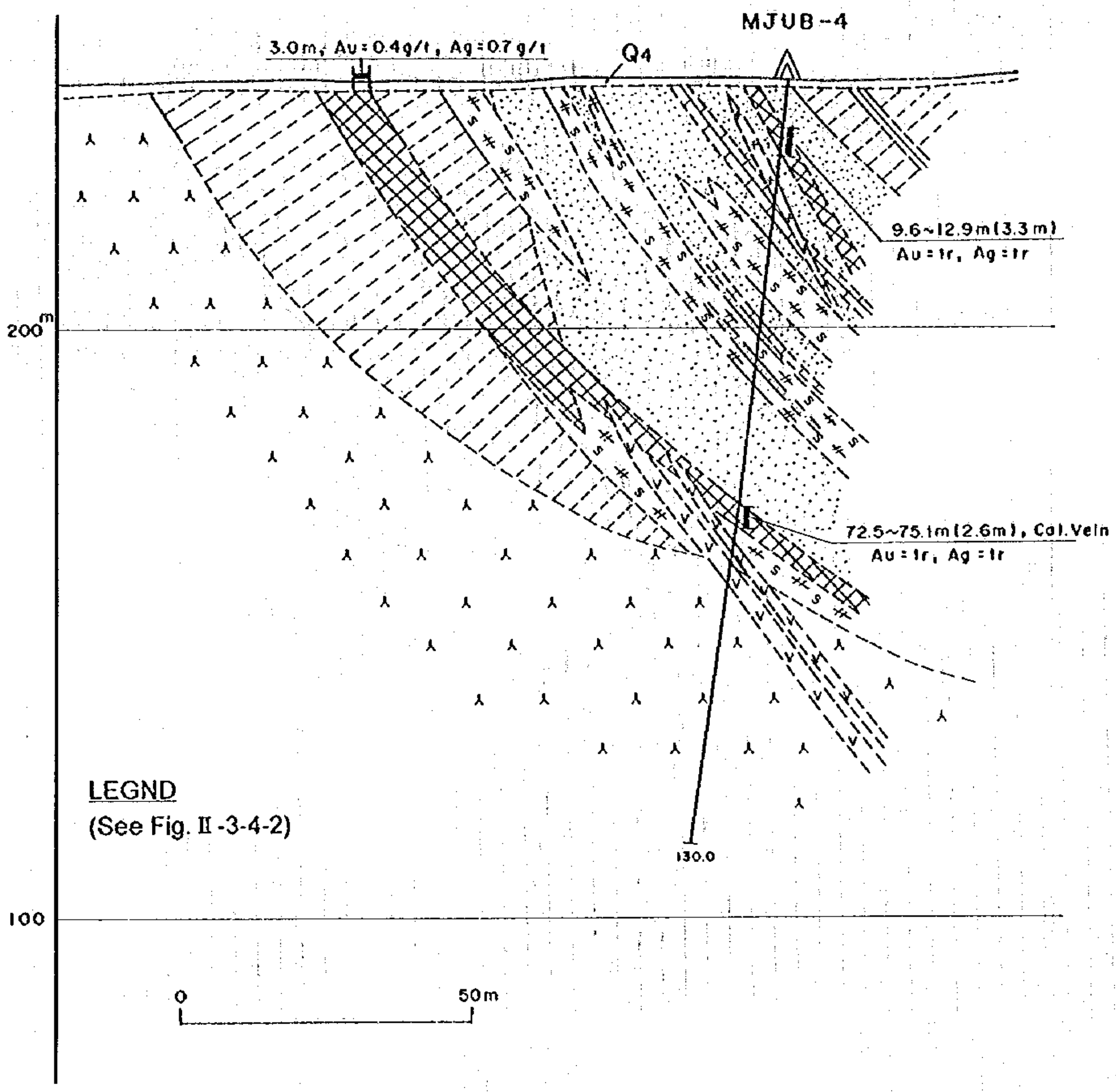

Fig. II－3－4－3　　Geological Cross Section along MJUB－4

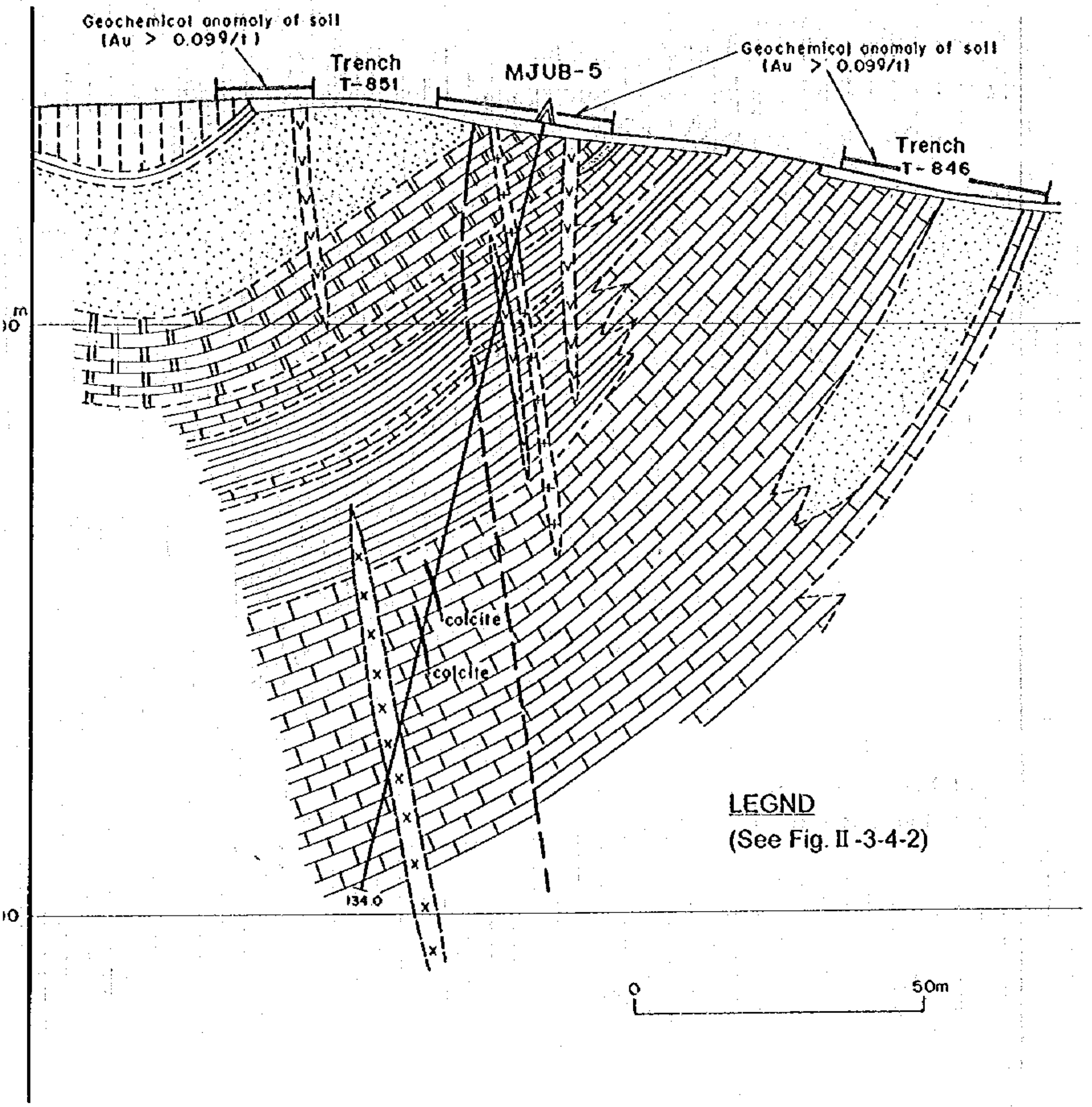

Fig. II−3−4−4 Geological Cross Section along MJUB−5

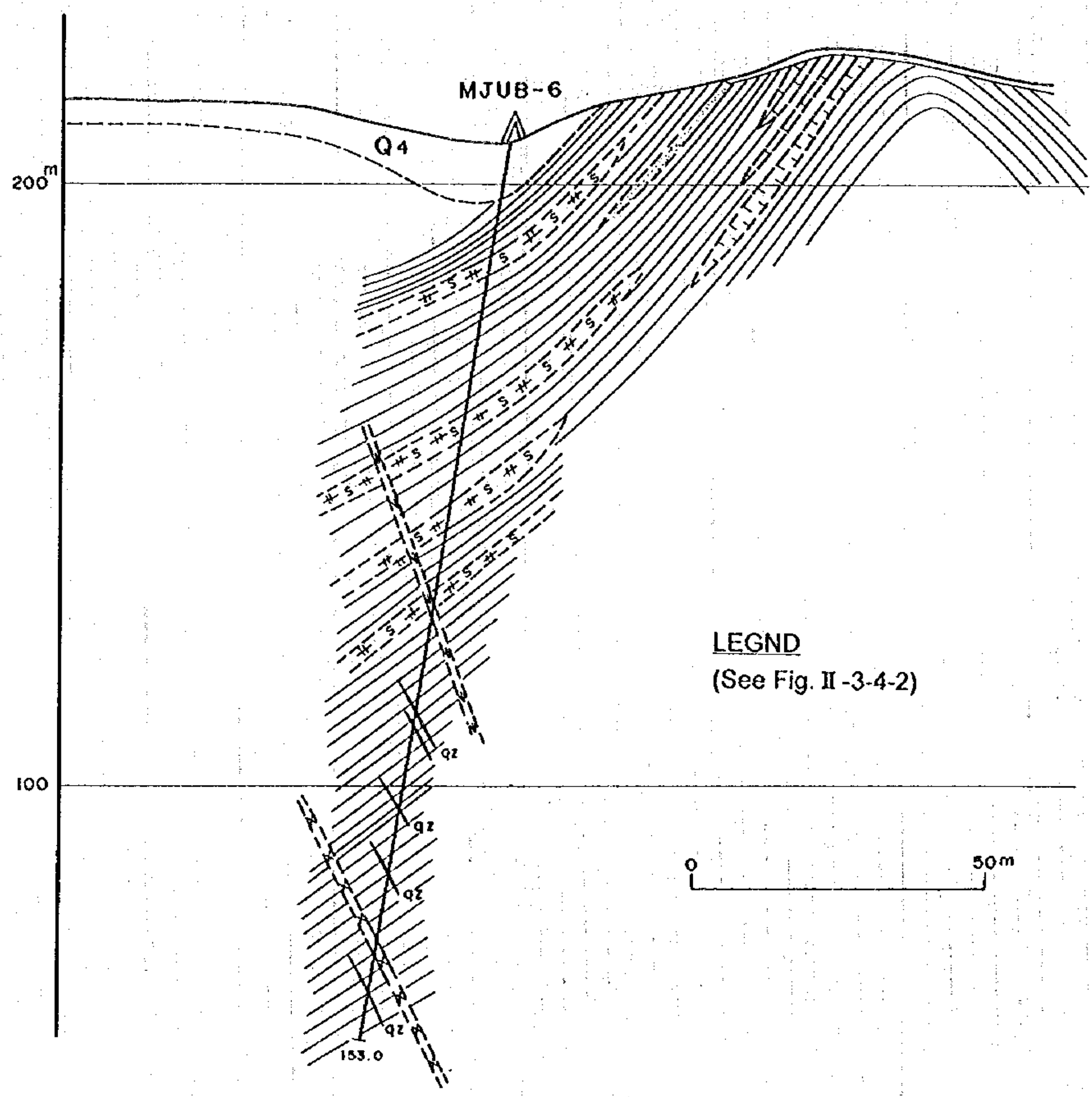

Fig. II−3−4−5 Geological Cross Section along MJUB−6

Table II-3-4-2 Efficiency of Each Drillhole in the Bulutkan District

Hole No.	Drilling Machine	Working Period	Drilling Length (m)	Core		Working Day			Efficiency		
				Length (m)	Recovery (%)	Drilling* (day*)	Others (day)	Total** (day**)	m/day*	m/day**	m/working period
MJUB-1	SKB−5P	July 19, '95 ↓ Sept. 11, '95	150.0	120.4	80.3	22.9	8.1	31	6.55	4.84	2.74
MJUB-2	SKB−5P	Sept. 11, '95 ↓ Oct. 5, '95	200.0	181.15	90.6	14.1	8.9	23	14.18	8.70	8.23
MJUB-3	SKB−5P	Oct. 1, '95 ↓ Oct. 24, '95	143.5	120.7	84.1	11.5	10.5	22	12.48	6.52	5.98
MJUB-4	SKB−5P	Oct. 6, '95 ↓ Oct. 28, '95	130.0	107.9	83.0	13.5	7.2	20.7	9.63	6.28	5.65
MJUB-5	SKB−5P	Oct. 29, '95 ↓ Dec. 15, '95	134.0	108.9	81.3	22.6	12.7	35.3	5.93	3.80	2.79
MJUB-6	SKB−5P	Oct. 27, '95 ↓ Nov. 13, '95	153.0	129.8	84.8	10.6	5.7	16.3	14.43	9.39	8.50
MJUB-7	SKB−5P	Nov. 14, '95 ↓ Dec. 6, '95	100.5	82.3	81.9	10.6	9.1	19.7	9.48	5.10	4.51
Total			1,011.0	851.15	84.2	105.8	62.2	168	9.56	6.02	4.72

* includes drilling and out drilling.

** includes drilling, out drilling, regain of accident, preparation, dismount/mobilization and others.

Table II-3-4-3 Working Time of Diamond Drilling in the Bulutkan District

Hole No.	Working Period		Number of Workers		Working						
	Period	(day)	Foreman (man)	Worker (man)	Drilling (hour)	Out Drilling (hour)	Regain of Accident (hour)	Preparation (hour)	Dismount/ Mobilization (hour)	Others (hour)	Total (hour)
MJUB-1	July 19. '95 ↓ Sept. 11. '95	54.7	93	105.5	315	235	134	28	24	8	744
MJUB-2	Sept. 11. '95 ↓ Oct. 5. '95	24.3	69	69	219	119	182	8	24	—	552
MJUB-3	Oct. 1. '95 ↓ Oct. 24. '95	24	66	72	195	81	180	24	32	16	528
MJUB-4	Oct. 6. '95 ↓ Oct. 28. '95	23	62	68	175	149	92	16	44	20	496
MJUB-5	Oct. 29. '95 ↓ Dec. 15. '95	48	106	112	215	328	257	48	—	—	848
MJUB-6	Oct. 27. '95 ↓ Nov. 13. '95	18	49	67	182	73	21	80	36	—	392
MJUB-7	Nov. 14. '95 ↓ Dec. 6. '95	22.3	59	77	164	89	155	32	32	—	472
Total	—	214.3	504	570.5	1.465	1.074	1.021	236	192	44	4.032

Table II-3-4-4 Consumable Drilling Articles in the Bulutkan District

Item	Specification	Unit	Quantity							
			MJUB-1	MJUB-2	MJUB-3	MJUB-4	MJUB-5	MJUB-6	MJUB-7	Total
Cement		kg								
Bentonite		kg	1,500				1,300			2,800
Clear mud		kg				500	3,100		300	3,900
Polyacrylicamide		kg	145			160	450		20	775
N1 mud water		m^3	122	184	120	95	120	75	88	804
N4 mud water		m^3	57			26	125		33	241
Diamond bit	76mm	pc	22	33	18	28	23	2		126
Diamond bit	59mm	pc	6		3		7	13	6	35
Diamond reamer	76mm	pc	2		1	2		1		6
Diamond reamer	59mm	pc	1		1			1	1	4
Metal crown	112mm	pc	10			16				26
Metal crown	93mm	pc					10			10
Metal crown	76mm	pc	32	11		4			10	57
Core box	56~58mm	pc	17	26	10	15	13	2	1	84
〃	36~40mm	pc	1		6		6	16	11	40

Table II-3-4-5 Drilling Meterage of Diamond Bits in the Bulutkan District

Size	Number of bits(pcs)	Drilling meterage by drillhole (m)							Total	Efficiency
		MJUB-1	MJUB-2	MJUB-3	MJUB-4	MJUB-5	MJUB-6	MJUB-7		m/bit
φ 76mm	22	125.1							125.1	5.69
	33		170.7						170.7	5.17
	18			95.4					95.4	5.30
	28				125.0				125.0	4.46
	23					92.6			92.6	4.03
	2						23.0		23.0	11.50
Sub total	126	125.1	170.7	95.4	125.0	92.6	23.0		631.8	5.01
φ 59mm	6	6.9							6.9	1.15
	3			48.1					48.1	16.00
	7					41.4			41.4	5.91
	13						130.0		130.0	10.00
	6							91.5	91.5	15.25
Sub total	35	6.9		48.1		41.4	130.0	91.5	317.9	9.08
Grand total	161	132.0	170.7	143.5	125.0	134.0	153.0	91.5	949.7	5.90

Table II-3-4-7 Major Mineralized Zones Caught by Drillings in the Bulutkan District

Hole No.	Depth (m)	True width (m)	Au (g/t)	Ag (g/t)	Cu (%)	Pb (%)	Zn (%)	As (%)	Bi (%)	Mo (%)	WO_3 (%)	Remarks
MJUB-1	80.3-81.0 (0.7)	0.4	1.4	tr	tr	tr	tr	0.62	tr	tr	tr	Silicified and skarnized metasomatite
	83.4-86.0 (2.6)	1.5	0.8	0.9	0.12	tr	tr	0.30	tr	tr	tr	Skarn and pyrite vein
	86.0-88.0 (2.0)	1.1	2.8	tr	0.06	tr	tr	0.01	0.01	tr	tr	Skarn
	92.0-95.0 (3.0)	1.7	0.5	1.1	0.05	tr	tr	0.13	tr	tr	tr	Skarn
MJUB-3	80.0-82.0 (2.0)	1.6	0.4	tr	tr	tr	tr	tr	tr	tr	0.02	Skarnized limestone and pyrite vein
	82.0-84.0 (2.0)	1.6	2.3	36.1	0.09	tr	tr	tr	tr	tr	0.02	Skarnized limestone
MJUB-7	0 -10.4(10.4)	5.5	4.3	1.1	0.05	tr	tr	0.03	tr	tr	tr	Silicified rock with drusey quartz, gossan and chalcedony
	10.4-15.6 (5.2)	2.8	0.4		0.05	tr	0.01	0.01	tr	tr	tr	Silicified rock with gossan
	15.6-16.6 (1.0)	0.5	0.6	2.8	0.08	tr	tr	0.04	tr	tr	tr	Silicified rock
	26.0-27.0 (1.0)	0.5	0.8	tr	0.10	tr	tr	tr	tr	tr	tr	Lamprophyre
	36.1-51.0(14.9)	7.9	21.2	4.3	0.07	tr	tr	0.09	tr	tr	tr	Skarn and skarnized sandstone
	52.1-66.5(14.4)	7.6	0.3		0.01	tr	tr	tr	tr	tr	tr	Silicified and skarnized metasomatite

PART III CONCLUSIONS AND RECOMMENDATIONS

Chapter 1 Conclusions

Following are the conclusions by district based on this fiscal year's survey.

1-1 Sautbay-Bulutkan District (Geological Survey Area)

(1) The survey area is dominated by the Karashakh Formation and the Kokpatas Formation both pertaining to the Ripheian ~ Vendian Systems of the Proterozoic. From the Late Carboniferous to the Early Permian, granodiorite around the Sautbay deposit, syenodiorite around the Bulutkan deposit and granitic rocks in the northeast of the survey area, respectively, intruded into the Proterozoic in the form of stocks. These rock bodies are accompanied by numerous dikes of dioritic rocks, lamprophyre and syenitic rocks. The dikes abound especially from the syenodiorite bodies of the Bulutkan deposit to the granitic rock bodies in the northeast of the survey area. In these strata and intrusive rocks, faults develop in the NW-SE, NE-SW and NNW-SSE directions.

(2) As regards the alteration zones around and to the west of Sautbay, among those extracted by the spectral analysis of the satellite imagery in the first year, it was ascertained by the geological survey that they are formed with sandstone and slate disseminated with limonite of the Kokpatas and Karashakh Formations, which are not those deriving from thermal process but reflecting the pyrite alteration zone accompanying diagenesis.

(3) This year's survey did not result in confirming occurrence of a new ore deposit or showings in the survey area, in addition to the known ore deposits at Sautbay (W), Burgut (W), Saghinkan (W) and Bulutkan (Au).

(4) Since the anomalies in the rock analysis are mostly located at or near the areas where stocks and dikes are concentrated, the mineralization is considered to extend over a wide area including the Bulutkan and Sautbay districts, accompanying intrusive rocks. In view of the fact that no correlations are recognizable between the elements and that anomalies of various elements are found within a small area, a plural number of polymetallic mineralization of different characters might have overlapped in the area.

The ore samples are generally in low grades, many of which did not reach the detestion limits. None of the ore samples showed significant grades.

1-2 Sautbay District

(1) Ore reserves of the Saghinkan deposit (W) was estimated, for which a computer software (MicroLYNX Plus) for ore reserve calculation was used in continuation from the first fiscal year. As the result, the ore reserve turned out to be 16,320,000t averaging 0.24% WO_3 and 0.02g/t Au, in case of a cutoff grade at 0.05% WO_3.

In case of a cutoff grade at 0.1% WO_3, ore reserves come to 13,944,000t averaging 0.27% WO_3, which is larger in ore reserves but lower in average grade when compared to the Uzbek-side estimation of 12,710,000t averaging 0.32% WO_3.

The WO_3 grades of skarn-type tungsten mines operated in the Western countries (USA, Canada, Australia, Korea, Turkey, etc.) since 1980 are over 0.5% in case of open-pit mining whilst, in case of underground mining, they are mostly over 1%. As occurrence of the ore bodies is as deep as 110-400m, the Saghinkan deposit would have to be exploited mainly by underground operation, which means its WO_3 grade is considerably lower than those of operating mines in the West.

(2) The drilling survey (four drillholes) at the Sautbay deposit ascertained that the No.1 ore body -- the main ore body -- strikes NNW-SSE and dips about 70°E and that the mineralization is continued up to about 400m below the surface in the southeast of MJUS-2.

Portions where WO_3 grades in excess of 0.30% were seized over 2m or more of true width were located at the No.1 ore body (true width 13.2m; WO_3 0.35%) captured between the depths of 319.8m and 338.5m of the borehole MJUS-3, the No.3 ore body (true width 2.3m; WO_3 2.31%) captured between 359.6m and 362.9m, and the No.1 ore body (true width 5.0m; WO_3 0.84%) captured between 309.3m and 315.8m of MJUS-4. In the light of the relationship between the locations of these bonanza and that of bonanza on the surface, the bonanza may be presumed to plunge in the SSE direction.

Therefore, the tungsten mineralization is highly likely to be continued downward and southeastward.